NPS-SP-22-003

NAVAL POSTGRADUATE SCHOOL

MONTEREY, CALIFORNIA

DESIGNING AND TESTING OF A 3D-PRINTED SPECIMEN FOR COMBINED LOADING

by

Clara Troeger

July 2022

Prepared for: Helmut-Schmidt-Universität Hamburg

THIS PAGE INTENTIONALLY LEFT BLANK

REPORT DOCUMENTATION PAGE

PLEASE DO NOT RETURN YOUR FORM TO THE ABOVE ORGANIZATION.

1. REPORT DATE	2. REPORT TYPE	3. DATES COVERED	
		START DATE	END DATE
7/14/2022	Technical Report	03/30/2022	07/14/2022

4. TITLE AND SUBTITLE
Designing and testing a 3D-printed specimen for combined loading

5a. CONTRACT NUMBER	5b. GRANT NUMBER	5c. PROGRAM ELEMENT NUMBER
5d. PROJECT NUMBER	**5e. TASK NUMBER**	**5f. WORK UNIT NUMBER**

6. AUTHOR(S)
2nd Lt (GER Army) Clara Troeger

7. PERFORMING ORGANIZATION NAME(S) AND ADDRESS(ES)
Department for Mechanical and Aerospace Engineering
Naval Postgraduate School
Monterey, CA, 93943

8. PERFORMING ORGANIZATION REPORT NUMBER
NPS-SP-22-003

9. SPONSORING/MONITORING AGENCY NAME(S) AND ADDRESS(ES)
Helut-Schmidt-Universität, Universität der Bundeswehr Hamburg
Fakultät für Maschinenbau
Professur für Mechatronik
Holstenhofweg 85
22043 Hamburg, Germany

10. SPONSOR/MONITOR'S ACRONYM(S)
HSU

11. SPONSOR/MONITOR'S REPORT NUMBER(S)

12. DISTRIBUTION/AVAILABILITY STATEMENT
Distribution Statement A: Approved for public release; distribution is unlimited

13. SUPPLEMENTARY NOTES
Thesis Examiners: Univ.-Prof. Dr.-Ing. Delf Sachau (HSU), Distinguished Prof. Young W. Kwon (NPS)

14. ABSTRACT
Failure prediction is of essential importance for everything built in today's world. Components are fabricated lighter and more specific in shape in order to fulfil their purpose. For reasons both of safety and stability, an exact prediction of the potential failure location and path is required. Recently new failure criteria were found for uniaxial loading. Since loadings are very seldom uniaxial but combined, a specimen for combined bending and torsion was designed and tested in a uniaxial testing machine. The specimens were 3D printed with polycarbonate and various modifications such as holes and different loading cases. The purpose of this is to verify if the failure criteria are applicable for combined loading as well. Comparing the experimental failure stress, location and path with the prediction made by the criteria the results are very similar. This allows the assumption that the failure criteria are also valid for combined loading.

15. SUBJECT TERMS
Combined loading, failure criteria, 3D-printing

16. SECURITY CLASSIFICATION OF:			17. LIMITATION OF ABSTRACT	18. NUMBER OF PAGES
a. REPORT	b. ABSTRACT	C. THIS PAGE		
unclassified	unclassified	unclassified	unclassified	68

19a. NAME OF RESPONSIBLE PERSON	19b. PHONE NUMBER *(Include area code)*
Clara Troeger	

STANDARD FORM 298 (REV. 5/2020)

THIS PAGE INTENTIONALLY LEFT BLANK

NAVAL POSTGRADUATE SCHOOL
Monterey, California 93943-5000

Ann E. Rondeau
President

Scott Gartner
Provost

The report entitled "Designing and testing a 3D-printed specimen for combined loading" was prepared for "Helmut-Schmidt-Universität Hamburg" and funded by the "German Armed Forces".

Distribution Statement A: Further distribution of all or part of this report is authorized.

This report was prepared by:

2nd Lieutenant Clara Troeger, German Army
B.Sc.

Reviewed by:

Young Kwon
Distinguished Professor
Mechanical and Aerospace Engineering

Reviewed by:

James Newman, Chairman
Space Systems Academics Group

Released by:

Kevin B. Smith
Dean of Research

THIS PAGE INTENTIONALLY LEFT BLANK

HELMUT SCHMIDT UNIVERSITÄT
Universität der Bundeswehr Hamburg

Master-Arbeit

Clara Tröger

Entwerfen und Testen eines 3D-gedruckten Prüfkörpers für überlagerte Beanspruchung

Designing and testing of a 3D-printed specimen for combined loading

Professur für Mechatronik

Master-Arbeit zum Thema:

Entwerfen und Testen eines 3D-gedruckten Prüfkörpers für überlagerte Beanspruchung
Bearbeitungszeitraum: 30.03.2022 – 30.07.2022

Clara Tröger
Matrikelnummer 893907
Maschinenbau
St.-Jahrgang 2018

Erstgutachter: Univ.-Prof. Dr.-Ing. Delf Sachau
Zweitgutachter: Distinguished Prof. Young W. Kwon

Professur Mechatronik
Fakultät Maschinenbau
Helmut-Schmidt-Universität / Universität der Bundeswehr Hamburg
Monterey, 2022

Acknowledgement

Professor Kwon has been a perfect mentor and thesis supervisor. Always offering advice and assistance as well as very interesting and outside the box conversation. I´m proud of and very grateful for the time I had the privilege to work with Professor Kwon.

Many thanks to my sister in crime, Chiara, who helped me through the jungle of Ansys and shared endless Cinnamon rolls with me.

Another big thank you goes to Professor Sachau giving me the opportunity to write the thesis in sunny California and who was even taking the trouble of flying over for the presentation. Here I want to include gratitude to both universities, the Naval Postgraduate School in Monterey and the Helmut-Schmidt-Universität in Hamburg for being my academic home.

A last thank you goes out to my family and friends that have always been beside me with their love and encouragement.

Task/Aufgabenstellung

Designing a specimen for combined loading with torsion and bending. Tests are conducted with a uniaxial testing machine. To achieve the desired combined loading, the design of the specimen needs to be adapted to the uniaxial machine. Beforehand simulation ensures that the failure occurs in the test area of the specimen. Due to 3D-printing, the design of the specimen is versatile and can be adapted to whichever requirements wanted. The specimen is printed with a brittle filament (polycarbonate) and will be tested to verify the design and the simulation. After a successful test, the effect of a hole in the testing area of the specimen will be tested. In addition, predictions on the location and the path of failure will be made by using Professor Young Kwon's theory about failure criteria for brittle material. This is to find out if the failure criteria are applicable for combined loading using a uniaxial testing machine.

Entwurf eines Prüfkörpers für eine überlagerte Beanspruchung von Torsion und Biegung. Als Prüfstand dient eine einachsige Zugprüfmaschine, auf die das Design des Prüfkörpers angepasst wird, um die gewünschte Beanspruchung zu erwirken. Durch vorherige Simulation wird sichergestellt, dass sich der Ort des Versagens im Testabschnitt des Prüfkörpers befindet. Da der Prüfkörper 3D-gedruckt wird, sind die Möglichkeiten im Design vielfältig und können spezifisch an die gewünschten Anforderungen angepasst werden. Die Prüfkörper werden mit Polycarbonat, einem spröden Filament, 3D-gedruckt und anschließend in der Zugmaschine getestet. Die Testergebnisse überprüfen und bestätigen den Erfolg des Designs und der Simulation. In einem weiteren Schritt wird der Einfluss einer kreisförmigen Aussparung im Prüfkörper getestet. Zusätzlich werden Vorhersagen über den Ort des Versagens und die Rissausbreitung gemachen gemäß der vom Betreuer Professor Young W. Kwon vorgestellten Kriterien zum Versagen spröder Materialien. Dabei soll geprüft werden, ob die Kriterien für überlagerte Beanspruchung anwendbar sind, wenn eine einachsige Zugmaschine genutzt wird.

Abstract/Kurzzusammenfassung

Failure prediction is of essential importance for everything built in today's world. Components are fabricated lighter and more specific in shape in order to fulfil their purpose. For reasons both of safety and stability, an exact prediction of the potential failure location and path is required. Recently new failure criteria were found for uniaxial loading. Since loadings are very seldom uniaxial but combined, a specimen for combined bending and torsion was designed and tested in a uniaxial testing machine. The specimens were 3D printed with polycarbonate and various modifications such as holes and different loading cases. The purpose of this is to verify if the failure criteria are applicable for combined loading as well. Comparing the experimental failure stress, location and path with the prediction made by the criteria the results are very similar. This allows the assumption that the failure criteria are also valid for combined loading.

Die Vorhersage von Materialversagen ist von grundlegender Wichtigkeit für das Auslegen von Materialien in der heutigen Zeit. Bauteile werden leichter und in Form spezifisch auf ihr Einsatzgebiet ausgelegt. Aus Sicherheits- und Stabilitätsgründen ist eine exakte Vorhersage von potenziellem Versagensort und -pfad nötig. Dazu wurden kürzlich neue Versagenskriterien für einachsige Belastungen vorgestellt. Da jedoch Belastungen selten einachsig, sondern überlagert auftreten, wurde ein Prüfkörper für überlagerte Biegung und Torsion entworfen und in einer einachsigen Zugmaschine getestet. Die Prüfkörper wurden mit Polycarbonat 3D-gedruckt, sowie mit verschiedenen Modifikationen, wie Löchern und unterschiedlichen Belastungsfällen. Zweck dieser Tests ist es, zu prüfen ob die Versagenskriterien auch auf überlagerte Beanspruchungen anwendbar sind. Der Vergleich der experimentellen Daten für Versagensort und -pfad mit den Vorhersagen, die mit den Kriterien getroffen wurden, ergibt eine große Ähnlichkeit. Dies lässt die Annahme zu, dass die Versagenskriterien auch für überlagerte Belastungen gelten.

Contents

Acronyms and abbreviations

FFF	fused filament fabrication
CAD	computer aided design
FEA	finite element analysis
PC	polycarbonate

List of symbols

Symbol	Meaning	Unit
A_0	original cross-sectional area	mm^2
E	Young`s modulus	$GPa\ (10^9\ N/mm^2)$
F	force/load	N
G	shear modulus	$GPa\ (10^9\ N/mm^2)$
I	second moment of inertia	mm^4
I_p	polar moment of inertia	mm^4
I_T	torsion constant	mm^4
l	length	mm
l_0	original length	mm
Δl	displacement/change in length	mm
M_b	bending moment	Nmm
s	distance along failure path	mm
T	twisting moment	Nmm
t	time	s
y	distance to neutral fibre	mm
ε	strain	mm/mm
ε_L	longitudinal strain	mm/mm
ε_T	transversal strain	mm/mm

κ_{fail}	failure value	*Pamm*
v	Poisson's ratio	-
χ	normalised stress gradient	*1/mm*
ρ	distance to neutral fibre	*mm*
σ	stress	*MPa (10^6 N/mm^2)*
σ_{fail}	Failure strength	*N/mm^2*
σ_{max}	maximum principal stress	*N/mm^2*
σ_{nom}	nominal stress	*N/mm^2*
σ_x	normal stress along x-axis	*N/mm^2*
σ_y	normal stress along y-axis	*N/mm^2*
τ_{xy}	shear stress	*N/mm^2*

1 Introduction

3D printing has become a major topic in research and industry over the past couple of years. It is used in many different fields such as health care, prototyping or optimising lightweight construction. Being such a flexible and independent technique, it´s of high interest to the armed forces around the world. Especially the navy can benefit from it a lot [1, 2]. A high readiness of action, power of endurance and independence are the crucial conditions for being successful in combat on board a warship. 3D printing increases all of these by enabling the crew to print spare parts or temporary solutions at an instant without having to wait days or even weeks for a supply ship or the next harbour. Because material properties vary between different printers, printer settings and used filament, there is no data base available for the material properties. This makes it unsafe and impossible to print spare parts that are safety related so far. Obtaining these material properties as well as predicting their failure must therefore be researched. To make the testing easier and more widely available, a design for combined loading using a uniaxial testing machine (normally used for tensile tests) is thought of and tested in this thesis. After a successful testing of the designed specimen, a two criteria theory for failure and failure path prediction will be verified. The theory has only been applied to uniaxial loading so far but will be applied to combined loading by comparing finite element analysis (FEA), analytic calculation and the actual test results. Confirming the theory for failure prediction and simplifying the testing for gaining material properties will make it possible to print spare parts that are safety related on board of warships. Other benefits will be e.g., shortening downtime in production, increasing safety and providing more creative and flexible solutions.

2 Theory

2.1 Tensile test

The tensile test is performed to determine the mechanical properties and fracture characteristic of a material by measuring its behaviour while force is applied [3]. Therefor a specimen is mounted on both ends in a uniaxial testing machine which pulls the specimen with a given, increasing load apart until it fails (Figure 1).

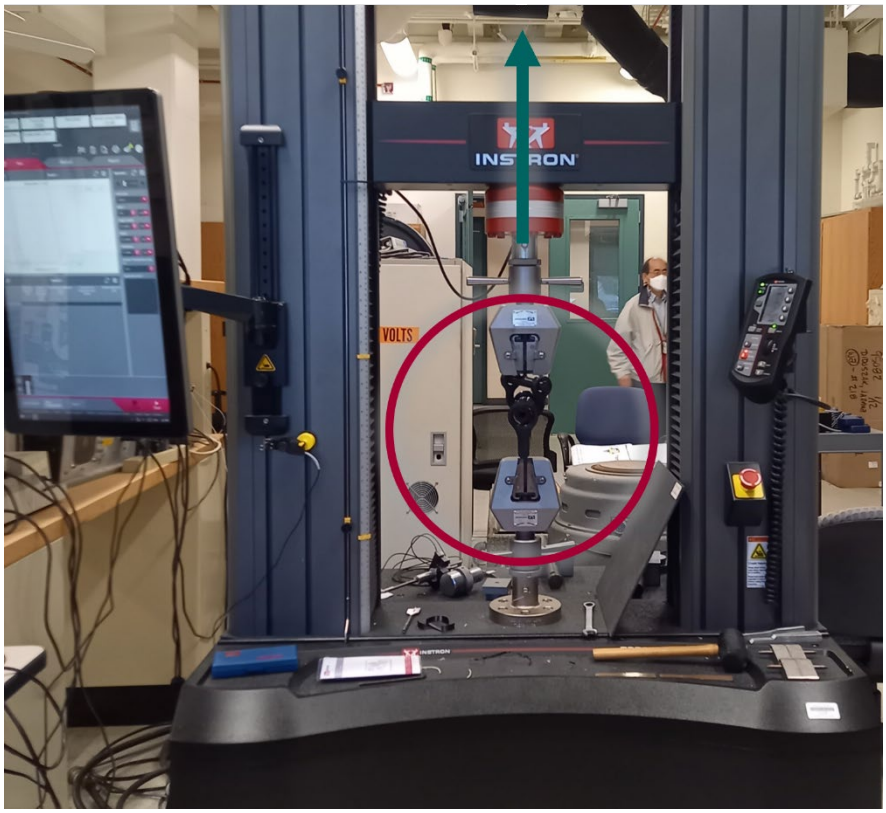

Figure 1: Instron® tensile machine

The load/force F is recorded as a function of the displacement Δl (increase in gage length) by a software. With this data and formula (1) and (2), the engineering stress σ and strain ε can be calculated.

$$\sigma = \frac{F}{A_0} \tag{1}$$

$$\varepsilon = \frac{l - l_0}{l_0} = \frac{\Delta l}{l_0} \tag{2}$$

Using engineering stress and strain neglects the changes in the cross-sectional area and the length during the tensile test. This is acceptable at low strains (elastic region) [4], which is the area of interest for this thesis. Out of this stress-strain curve the mechanical properties such as the ultimate tensile stress, the yield strength, which separates the elastic and the plastic region, and the Young`s modulus can be either determined or calculated [5] as shown in Figure 2.

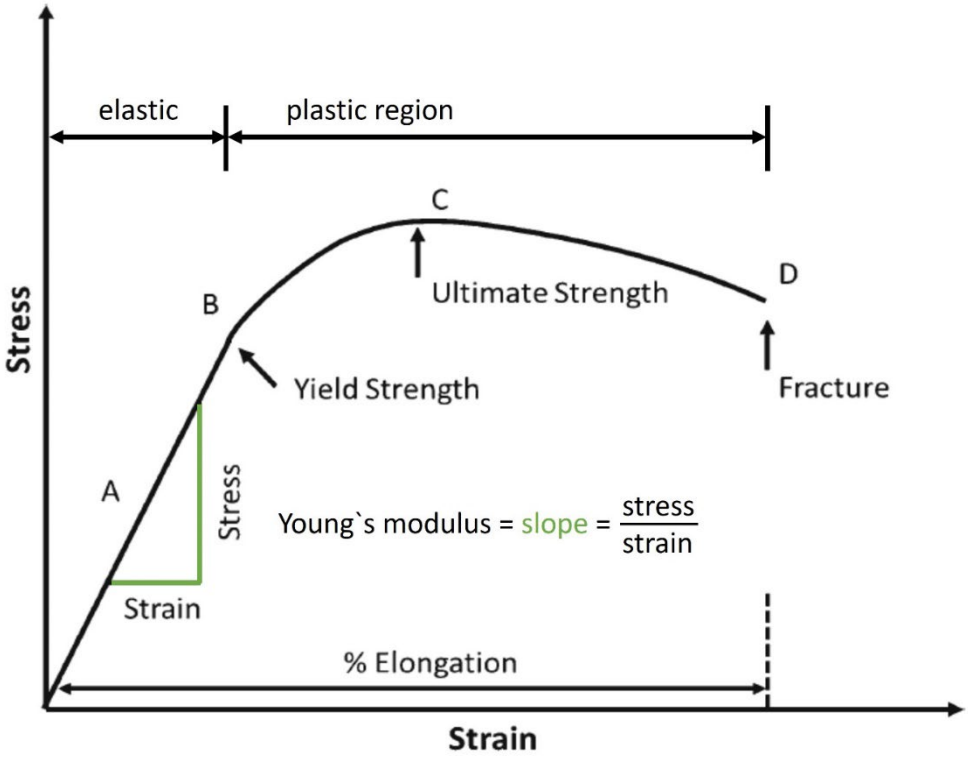

Figure 2: stress strain curve [6]

The Young`s modulus E can be read off the slope of the linear part of the stress-strain-curve (formula (3))

$$E = \frac{\sigma}{\varepsilon} = \frac{F}{A_0} \cdot \frac{l_0}{\Delta l} \qquad (3)$$

2.2 Strain gauges

Strain gauges are used to determine the strain of a material while tension or compression is applied. Figure 3 shows the build-up of a strain gauge. A resistance wire, arranged in a grid and fixed on foil is applied on a specimen parallel to the direction of the desired strain [7]. To determine the strain in various direction, a rosette can be used, where strain gauges are arranged in different angels (Figure 4).

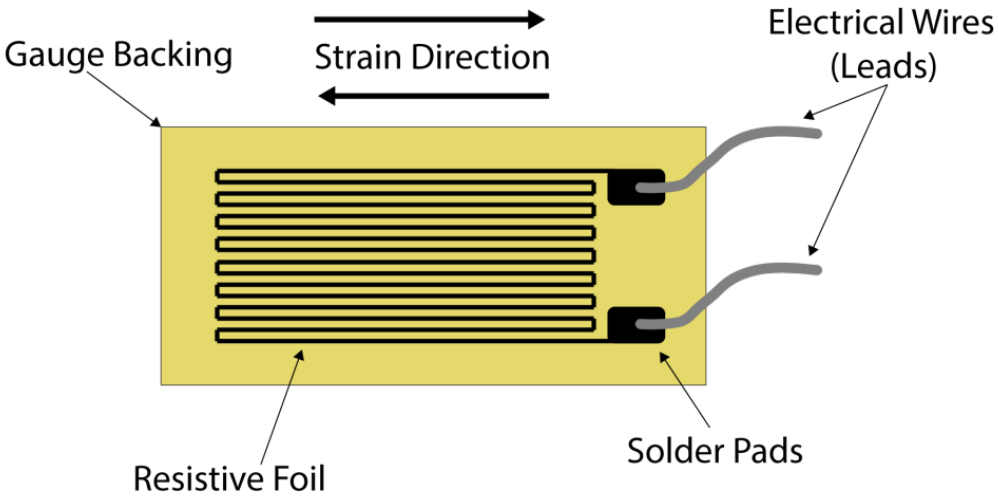

Figure 3: built-up of a strain gauge [8]

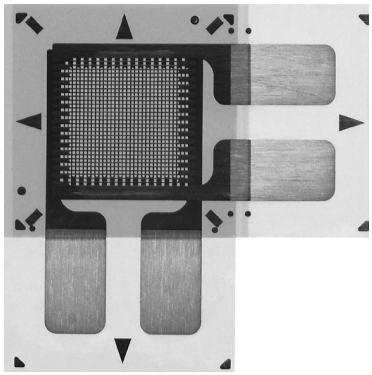

Figure 4: used strain gauge (rosette) [9]

A voltage is applied to the strain gauge, which is connected to a Wheatstone bridge (quarter bridge), that detects the change in resistance while pulling or compressing a specimen (tensile test). By applying tension, the specimen and the wire are getting stretched. As the length of the wire increases, the resistance increases, which is detected by the Wheatstone bridge [10]. The change in resistance/output voltage correlates directly to the strain [11]. Because the strain gauge has a specified

resistance at rest, which increases under strain, a ratio of that change in resistance, called gauge factor, must be included in the calculation [12].

With the transversal and longitudinal strain of a specimen, another important mechanical property, the Poisson`s ratio, can be determined (formula (4) [13]).

$$\nu = -\frac{\varepsilon_T}{\varepsilon_L} \tag{4}$$

With Young´s modulus and Poisson´s ratio, a third important material property, the shear modulus G, can be calculated according to formula (5). This formula only applies to isotropic materials [14].

$$G = \frac{E}{2(1+\nu)} \tag{5}$$

2.3 3D printing

For reasons of independents and flexibility of design, a 3D-printer was used to print out the specimens. The technical term for 3D-printing is additive manufacturing and the technique used in this thesis is called fused filament fabrication (FFF). Knowledge and experience in the wide range of printer settings is needed to get good print results and avoid the risk of defects or failure.

2.3.1 Basic concept and fused filament fabrication

Figure 5 shows the steps of the **basic concept** of 3D-printing from the imaginary idea to the actual 3D-printed object.

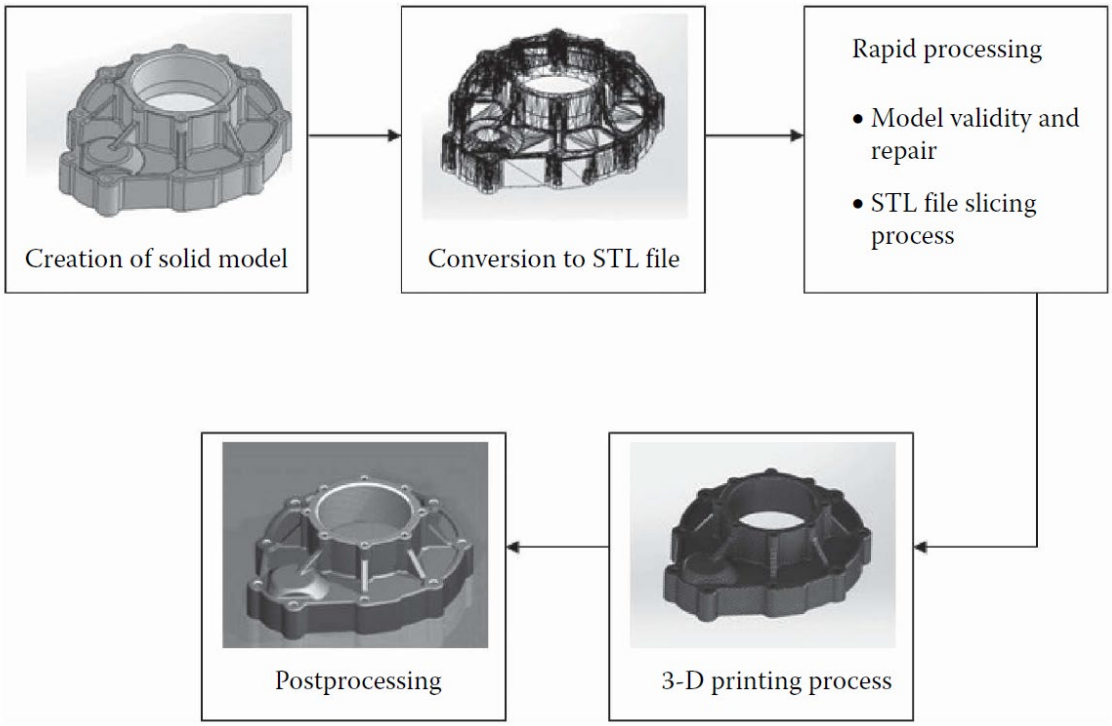

Figure 5: basic concept of 3D-printing [15]

First step: creating a 3D object, using a CAD (computer aided design) software.

Second step: converting the 3D model into an STL-file (represents the object as a series of triangles) [15].

Third step: A so called slicer-software cuts the model into horizontal cross-sectional layers and creates a path for the printer head to follow for each layer. The software often also controls the printer settings, such as layer thickness, printing temperature and the additional use of support structure.

Forth step: The object gets printed by adding layers on top of each other (like building a brick wall) until a three-dimensional object appears.

Fifth step: The model gets postprocessed by removing the support structure, redrilling holes or treating the surface.

Fused filament fabrication:

As the name already implies, FFF creates a 3D-object by fusing filament together. Therefore, the filament is provided by a spool and fed through into the printer head (Figure 6). This printer head includes a motor, that pushes the filament forward to a heated nozzle, which melts it. The applied heat puts the filament into a semiliquid state, so it can be deposited in thin layers [16]. The printer head then moves along a given path (step 3 and 4 of the basic concept) to create a 3D object. As soon as the molten filament is laid down onto the previous layer or the building plate, it cools down and fuses with the other layers, creating a solid part. For printing in mid-air (e.g. bridges) a support structure is needed, which is less dense and has to be removed afterwards. The support structure can be added and modified in the slicer and is a part of each printed cross-sectional layer.

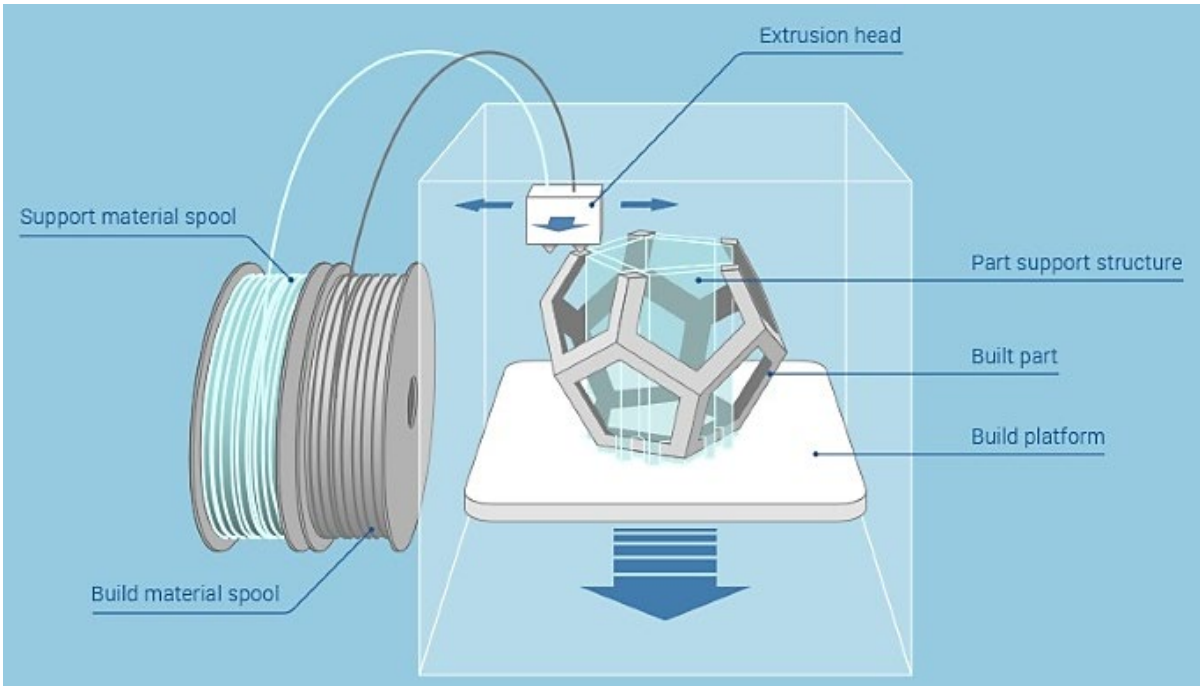

Figure 6: 3D - printing using fused filament fabrication [17]

2.3.2 Failure and troubleshooting

There are a few common problems while 3D printing, which can cause failure or result in bad quality. Some of them can be avoided by the right handling while others have to be solved by gradually adjusting the printer settings.

One of the most important things to make sure of is the proper storage of the filament. Companies like Ultimaker© recommend storing the filament in a resealable bag, out of direct sunlight and in a dry and cool place [18]. Because the filament is hygroscopic and decreases in quality by absorbing moisture, the print might fail and changing the printer settings won`t help.

Once the filament is extruded, it cools down and, as most materials, shrinks. This can cause two problems called warping and cracking. The shrinkage mainly depends on the used material and the difference between the nozzle and the environmental temperature. The higher the temperature gradient the higher the shrinkage [19]. When a new layer is added on top and cooled down to fast, it shrinks and causes the layer underneath to slightly bend upwards on the edges. This happening layer after layer can lead to a visible bend that detaches a layer either from the printing bed (warping) or the layer below (cracking) as shown in Figure 7.

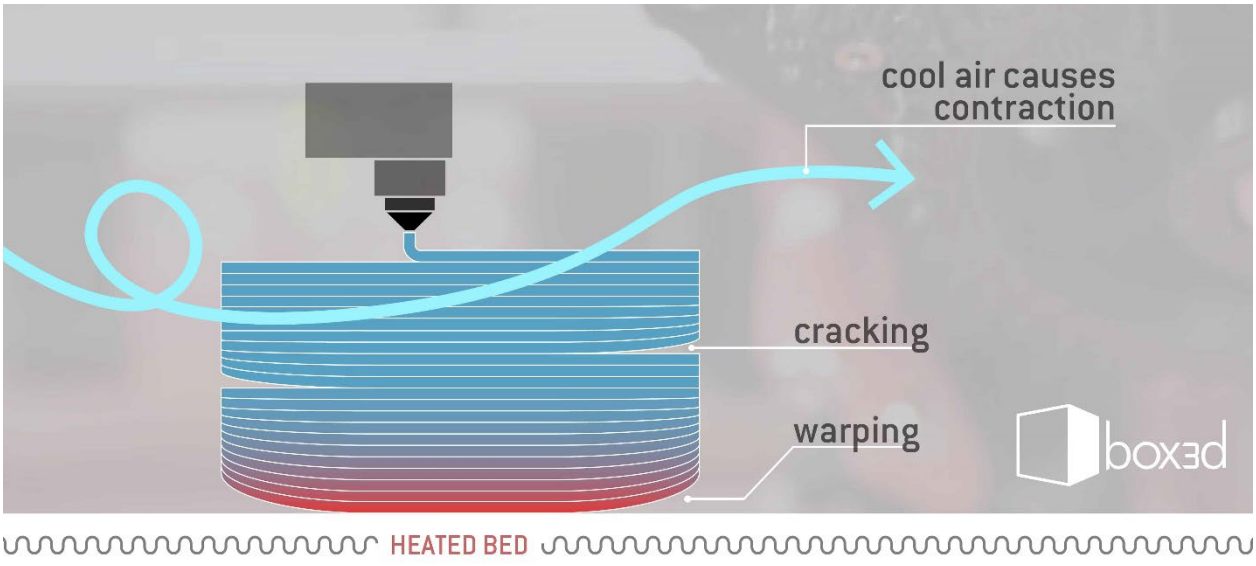

Figure 7: cracking and warping [19]

If warping occurs, the part can detach from the building plate and is free to move, which will lead to printing failure. Cracking on the other hand can not only cause a crack, but

can lead to residual stress within the part, which will decrease the strength of the part even if a crack can´t be seen. If a load is applied, failure will occur in the part where the residual stress is the highest.

To prevent those failures a few printer settings can be adjusted. Warping can be eliminated by the right temperature of the printing bed, which is usually pre-set by the slicer/printer according to the manufacturer. Especially with only a small area of the part touching the printing bed a brim can be added to increase the adhesion and decrease the risk of warping (Figure 8).

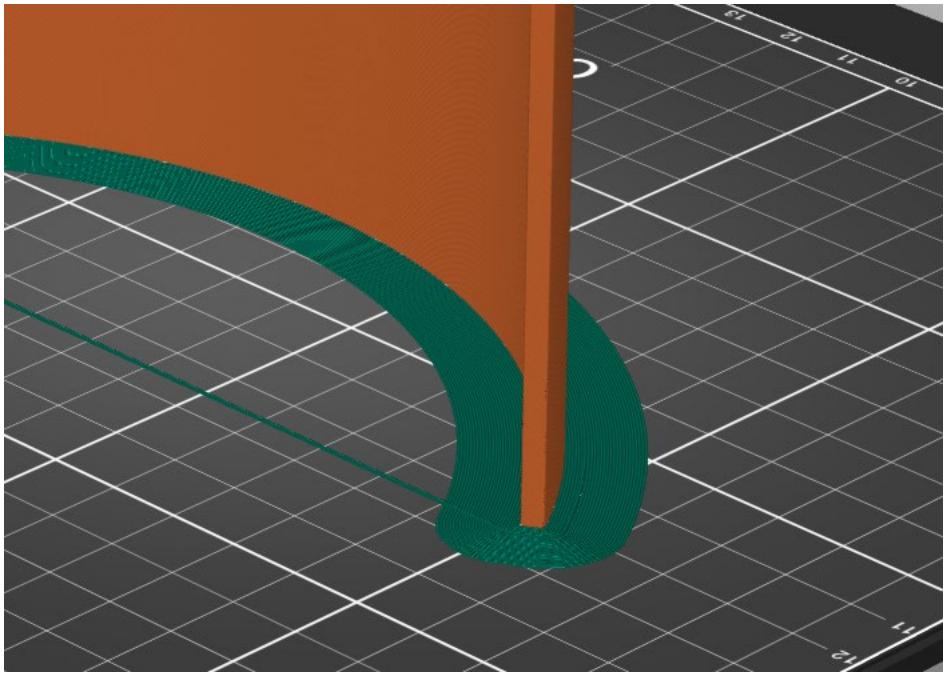

Figure 8: preview of a 3D printed part (orange) with a brim (green)

Cracking on the other hand can be avoided by decreasing the temperature gradient between the nozzle and the environment. Since the nozzle temperature is dictated by the used filament and pre-set by the manufacturer as well, the environmental temperature must be increased [20].

2.4 Finite element analysis (FEA)

The finite-element-analysis constitutes a numerical solution for partial differential equations, that describe space- and time-depended problems in engineering or applied science [21]. This solving method is used for problems where analytic solving is too complex or not possible such as the deformation of materials by crashing or modelling the stall for the wings of an aeroplane. The basic concept of FEA is to divide a continuous domain into small and simple, so-called finite elements (discretisation) with known boundary conditions or acceptable simplifications so that the equations can be solved. By assembling the similar properties of the finite elements per node, the characteristics for the whole problem can be estimated [22]. Figure 9 shows the mesh created by discretisation and the solution for the stress-allocation of a tensile test simulation.

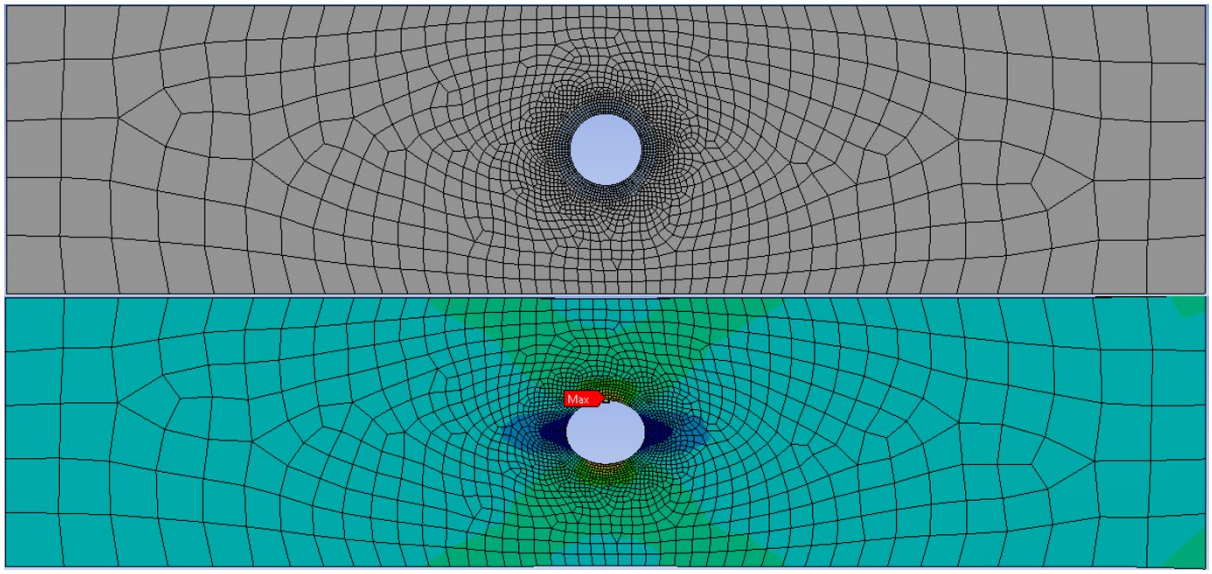

Figure 9: created mesh and stress-allocation after tensile test simulation (Ansys)

2.5 Combined loading

Usually, a part isn`t exposed to just one sort of load but to different types as well as loads in various directions. To determine the actual stress that occurs, different stresses can`t simply be added but must be weighted according to a chosen theory.

For combining bending and torsion, each individual stress must be estimated first. Using the bending moment M_b (formular (6)) the distance to the neutral fibre y and the second moment of inertia I (formula (7)), the bending stress can be calculated with formula (8).

Bending moment:

$$M_b = Fx \tag{6}$$

Second moment of inertia for a tube:

$$I = \frac{\pi}{4}(r_o^4 - r_i^4) \tag{7}$$

Bending stress:

$$\sigma_x = \frac{M_b y}{I} \tag{8}$$

Like the bending stress, the shear stress (formula (11)) is estimated with the twisting moment T (formula (9)), the distance to the neutral fibre ρ and the torsion constant I_T (formula (10)), which, for tubes, is the same as the polar moment of inertia.

Twisting moment:

$$T = Fr \tag{9}$$

Torsion constant/polar moment of inertia for a tube:

$$I_T = I_p = 2I \tag{10}$$

Shear stress:

$$\tau_{xy} = \frac{T\rho}{I_T} \tag{11}$$

As mentioned, the different stresses can`t simply be added. Therefore, the maximum stress theory is used to take both the normal and the shear stress into account. The maximum principal stress is calculated as shown in formula (12).

Maximum principal stress:

$$\sigma_{max} = \frac{\sigma_x + \sigma_y}{2} + \sqrt{\frac{(\sigma_x + \sigma_y)^2}{4} + \tau_{xy}^2} \tag{12}$$

Because the bending load for the combined loading is uniaxial ($\sigma_y = 0$) formula (12) can be simplified to formula (13).

$$\sigma_{max} = \frac{\sigma_x}{2} + \sqrt{\frac{\sigma_x^2}{4} + \tau_{xy}^2} \tag{13}$$

2.6 Prediction of failure

For predicting the failure for brittle notched specimens two criteria must be met [23]. The first one states that the maximum stress must be greater than the failure strength of the material and gives a first indication to where the potential failure location is (formula (14)).

$$\sigma_{max} \geq \sigma_{fail} \tag{14}$$

The second criterion that must be met describes the failure path along the greatest value for the cubic failure stress divided by the stress gradient along the failure path. It also includes the two material constants Young´s modulus and the failure value κ_{fail} (formula (15)).

$$\frac{\sigma_{fail}^3}{\left|\frac{d\sigma}{ds}\right|} \geq 2E\kappa_{fail} \tag{15}$$

Taking a closer look, the second criterion states that failure will occur along a path, the smaller the stress gradient is along that path. So, if a fibre is exposed to high stress but the ones next to it aren´t (high stress gradient) the neighbour fibres can support the high stressed fibre, so that overall the material won´t fail.

The stress gradient χ is normalised to the maximum stress and can be determined as shown in formula (16). The index i describes the node where the maximum stress occurs and i+1 the neighbour node in the direction of the least loss in stress.

Stress gradient χ:

$$\chi = \frac{1}{\sigma_{max,1}} \left| \frac{\left(\sigma_{max,i} - \sigma_{max,i+1}\right)}{s_{i+1} - s_i} \right| \tag{16}$$

3 State of the art

Combined loading:

Determining material properties is a well-researched and well-understood topic. There are multiple machines available for bending, torsion, shear stress or any combination of different loads. Usually, a specimen has to fit a certain normed size to get tested and most machines are only fit to do one type of loading. To be able to use a uniaxial machine for combined loading will open a wide range of new possibilities. This hasn`t been done so far because it required 3D printing, which has only recently become a prominent topic for research. The properties of 3D printed parts vary a lot between different printers and different printer settings, which makes it even more important to gain the material properties more easily. The greatest advantage is that 3D printing allows unique designs that can be adjusted easily.

Material properties of 3D-printed specimens (polycarbonate):

The main sources of influence on the strength of 3D-printed specimens apart from printer settings (layer thickness, printing temperature, etc.) are the printing direction and the printing angle (raster orientation) as shown in Figure 10. Testing polycarbonate specimens under cyclic loading showed that the flat and on-edge samples exhibit a way longer cyclic fatigue life than the up-right samples. This is because the load for flat and on-edge samples is carried by the infill- and wall-layers. On the other hand, as for the up-right specimen the load is carried by the bond between the layers [24, 25]. For static loads the printing angle and direction also have an influence on the material strength. Looking at flat printed out samples both, Younge´s modulus and Poisson´s ratio, increase slightly with the change of the infill-angle. Young´s modulus is 1620 MPa for 0°/90° while Poisson´s ratio is 0.29. For the angle +45°/-45° Young´s modulus is 1890 MPa and Poisson´s ration 0.39 [26].

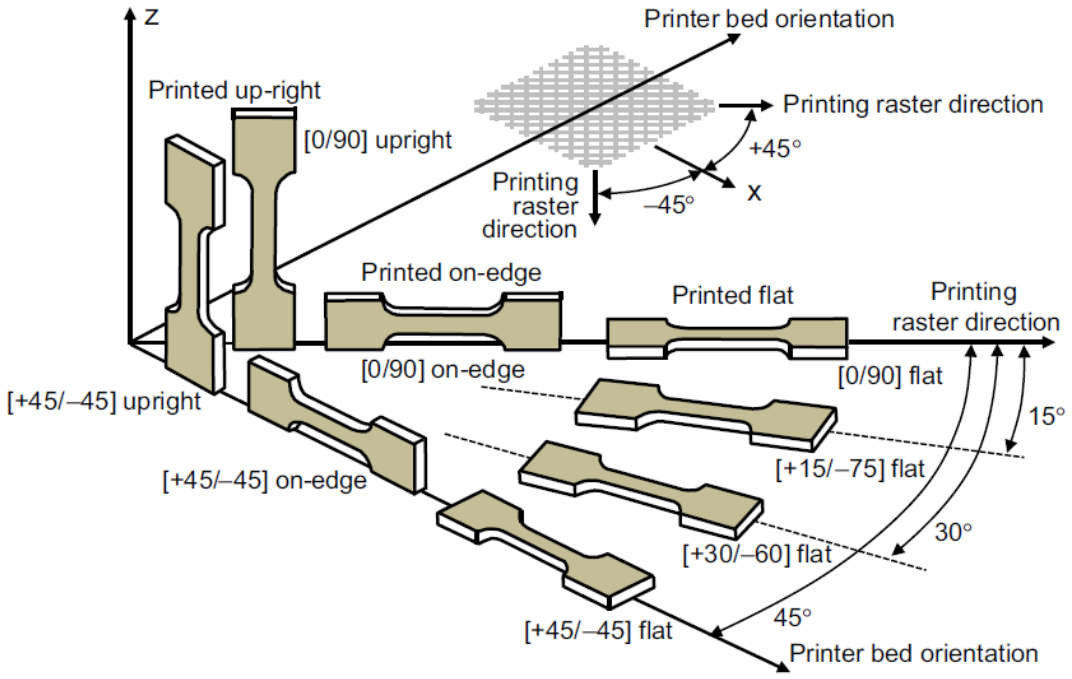

Figure 10: printing orientation and angle (raster orientation)

Failure prediction and criteria for brittle material:

To get a first approximation of where and when failure will occur, static hypothesis such as von Mises stress or the maximum normal stress criterion are used. For accurate failure prediction these theories are too limited and therefore have to be amplified or replaced. Since the prediction of the location and the path of failure are of high interest, a lot of research has been done. The middle-curve-criterion for example is used to predict fatigue life for combined loading of bending and torsion using one constant material parameter, determined out of experiments [27]. Another approach for curved three-dimensional frame elements divides the element into regions with 1D, 2D and 3D material response. This model is able of accurate failure prediction of a wide range of cross-section geometry but has its limits by combined loading of bending/axial load and shear stress [28]. To predict the failure path of a brittle material with pre-existing cracks an algorithm was used, that identifies the cracks, that most likely will from a large crack. By comparing it with a high-fidelity fracture simulation the time could be reduced by ≈ $O(10^6)$ [29]. Another promising attempt to predict failure for brittle material demands that two criteria must be met in order for the material to fail but predicts the failure path at the same time [23]. This theory has only been verified for uniaxial loading but will be tested for combined loading in this thesis.

4 Methods and results

To design a 3D printed specimen for combined loading (bending and torsion) by using a uniaxial tensile machine the following path was chosen. First an idea had to be born on how the design is going to look like. To make sure that failure occurs in the testing area of the specimen a finite-element-analysis is used to predict the location of the highest stress level. Therefore, the material properties like Young´s modulus, Poisson´s ration and the shear modulus have to be determined to set up a material for calculation. These properties can be obtained by a tensile test using strain gauges. To gain these values in the different material directions a dog shaped specimen for tensile testing was printed out with the layers being in an 0°, +45°/-45° and an 90° angle. Now the designed specimen is tested in a uniaxial tensile machine by applying increasing load until failure. The detected failure load is then used to compare the calculated maximum stress with the result of the FEA. Provided that both values match each other, the FEA can be claimed as valid. In the next step specimens with a 6 mm hole are tested and the maximum stress calculated with FEA. Calculating the stress gradient from the greatest maximum stress location and comparing it with the actual path of the failure will verify the second failure criterion [23].

4.1 Material properties of 3D-printed PC

4.1.1 Young`s modulus

To determine the Young´s modulus of 3D printed polycarbonate an Instron® tensile machine was used, and a displacement/increasing force of **2 mm per minute** was set up. After securing the specimen into the machine (Figure 11), it was set to a zero displacement and a balance of force. By starting the test, the tensile machine slowly pulls the specimen apart until it fails, while detecting the displacement as a function of time.

Figure 11: specimen(white) loaded into the tensile testing machine (Instron®)

For determining the material properties of 3D printed polycarbonate, 3 different dog-shaped specimens were used. One with a printing direction of 0º angle, one with 90º and one with +45º/-45º rotating as shown in Figure 12. All were printed out with the Ultimaker© S5 using black polycarbonate (brand: Ultimaker©).

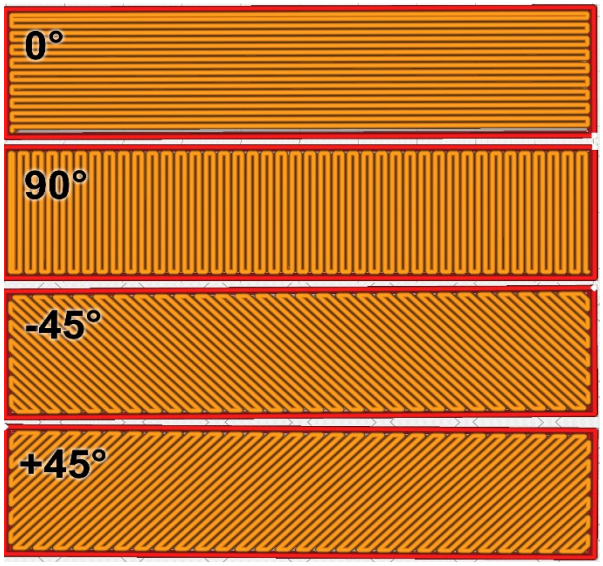

Figure 12: specimens with different printing direction

For 0° and 90° the layer on top has always the same direction as the one underneath. For 45° every other layer is rotated by 90° so they criss-cross. The test section in the designed specimen is printed without criss-crossing, so all layers have the same direction. The 0°-specimen covers two directions in space, because it is rotationally symmetric in the direction of the applied load for testing. The 45° sample was printed to verify the results. Figure 13 shows the stress-strain-curve of the three printing directions while Table 1 shows the Young´s modulus.

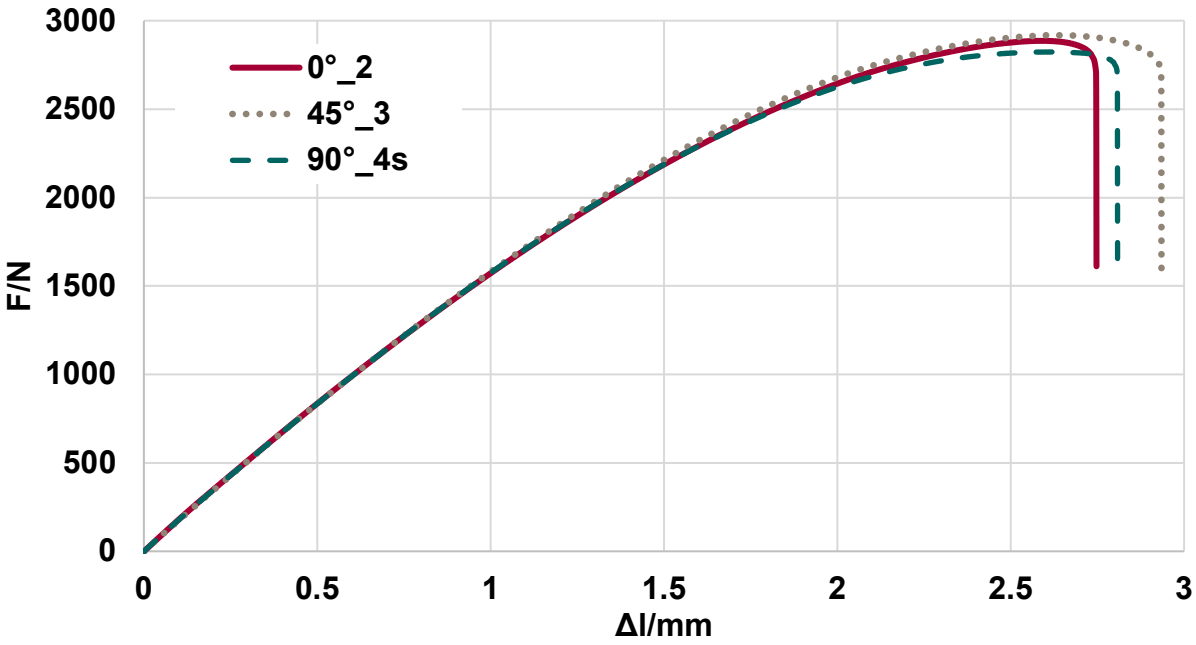

Figure 13: stress-strain-curve of the three printing directions

Table 1: Young´s modulus (GPa) for the three printing directions

sample	**0°**	**90°**	**45°**
1	1686,4	1574,1	1464,6
2	1702,4	1637,4	1516,3
3	1783,3	1524,3	1553,7
4	1684,2	1518,8	1582,6
average	**1714,1**	**1563,7**	**1529,3**

Value used for modelling (FEA): 1627,67 GPa

The value of the Young´s moduli as well as the stress-strain-curves are very similar, which allows the assumption to treat the 3D printed polycarbonate as an isotropic material.

The Young´s modulus along with Poisson´s ration and the shear modulus are needed to set up the material for the FEA with Ansys. Samples 3 and 4 for 0° and 90° were used to determine these three properties, because they had strain gauges attached for further measurements as described in the following chapter.

4.1.2 Poisson`s ratio

Using the same machine and the same settings described in chapter 4.1.1, the Poisson´s ratio for 3D printed polycarbonate was determined. Therefore, strain gauges were applied to the centre of the samples, cleaning and smoothing them first. In a second step wires were soldered to the strain gauges and connected to a Wheatstone bridge (normal resistance measured, as given by the manufacturer: 350 Ω). Figure 14 shows the linear part of the measured strain in longitudinal and transversal direction over time. Using the slopes of both curves the Poisson´s ratio can be calculated. Table 2 shows the results, which are all very similar as expected and which confirms the assumption of an isotropic material.

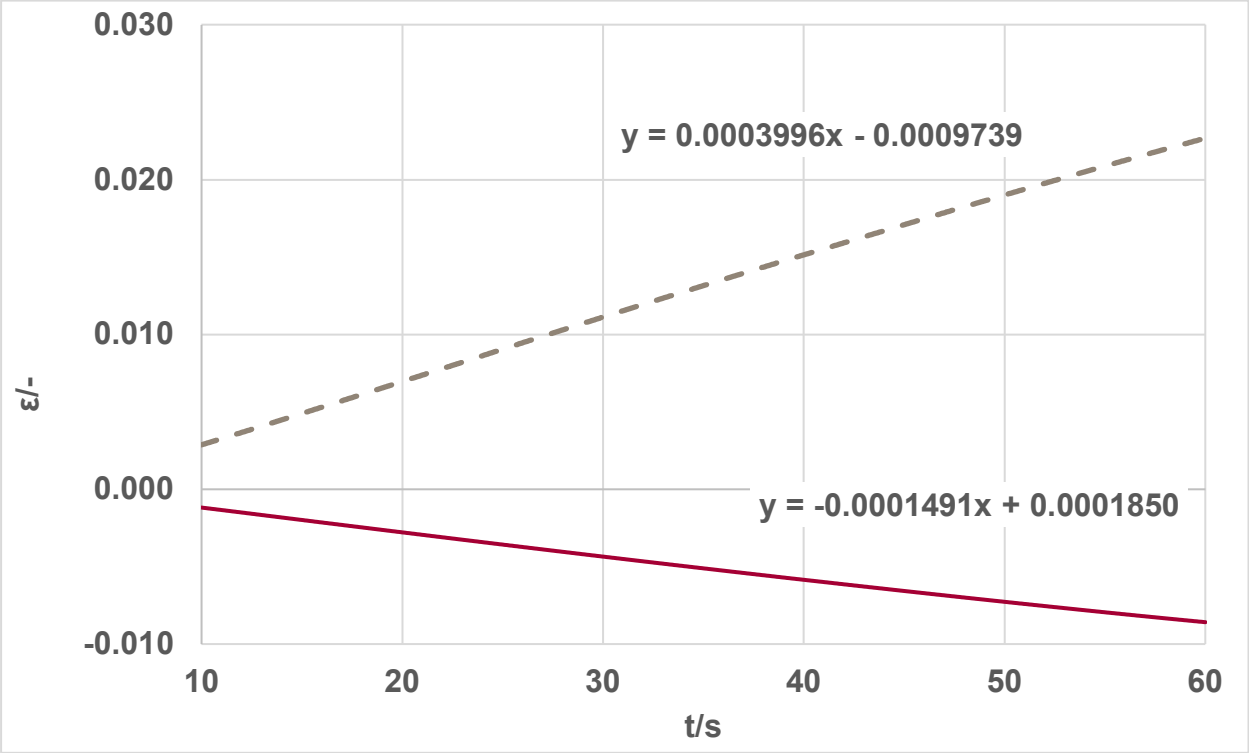

Figure 14: strain gauges result for 90°_4, showing the longitudinal (grey, broken curve) and transversal (red) strain

Table 2: Poisson´s ratio

sample	0°	90°
3	0,3735	0,3835
4	0,3703	0,3730
average	**0,3751**	

Because 3D printed polycarbonate is an isotropic material formula (5) can be used to determine the shear modulus. Results are shown in Table 3.

Table 3: Shear modulus in GPa

sample	0°	90°
3	649,2	550,9
4	614,5	553,1
average	**591,9**	

With the Young´s modulus, Poisson´s ratio and the shear modulus, a material, in this case the 3D printed black polycarbonate from Ultimaker©, can be set up for FEA-modelling using the software Ansys [30].

4.2 Designing, printing and testing of a combined loading specimen

4.2.1 Designing and printing

The first idea of a design for a specimen that can be loaded with bending and torsion at the same time using a uniaxial tensile testing machine was a one-piece design as shown in Figure 15. To decrease the long printing time, parts of the design are hollow. In addition, the originally planned dimensions were decreased by 50 % which reduced the printing time from three and a half days to 21 hours.

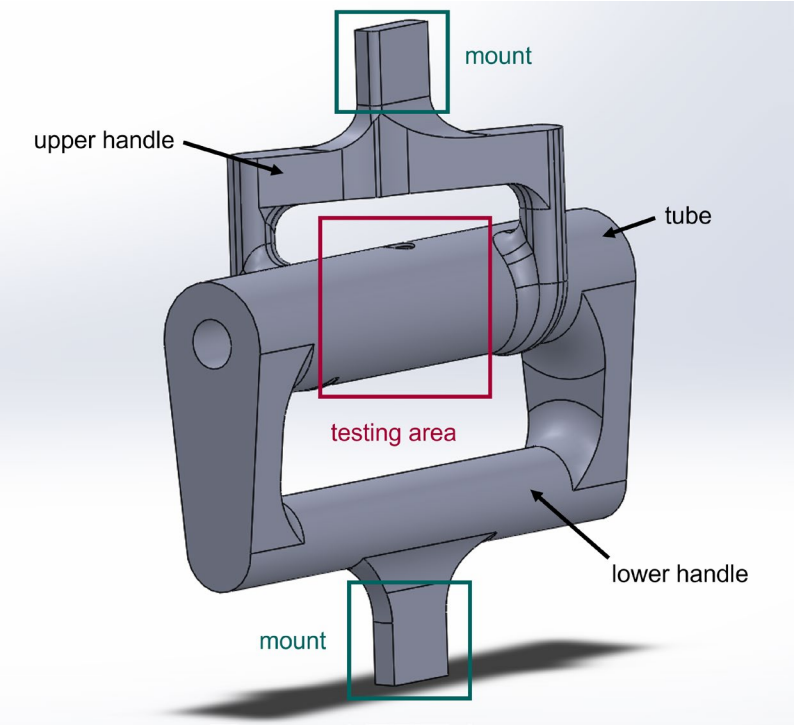

Figure 15: first design

The upper handle attached to both sides of the tube is responsible for applying torsion. In combination with the lower handle also bending is applied to the test section, as demonstrated in Figure 16.

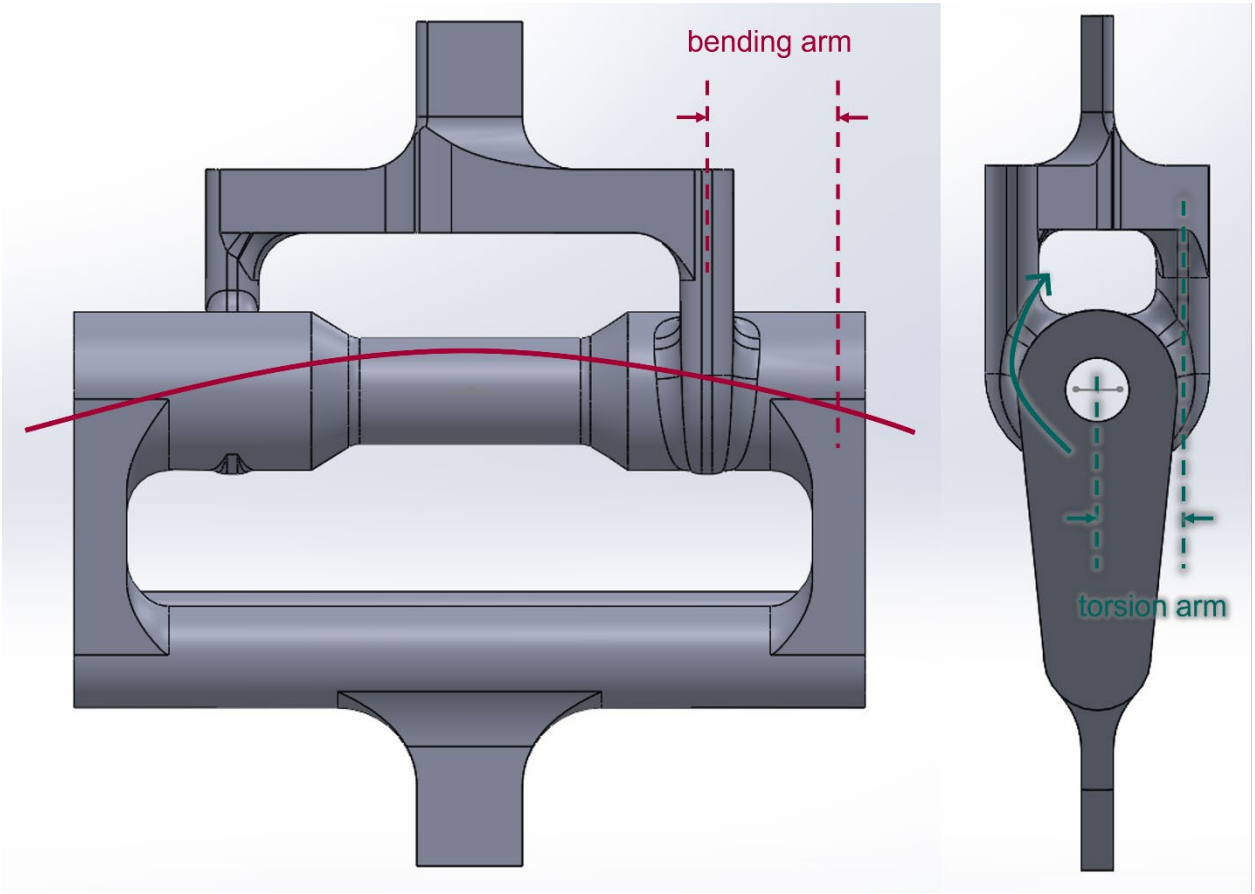

Figure 16: first design with the applied bending and torsion

The stress allocation of the design was also determined with FEA using Ansys as shown in Figure 17.

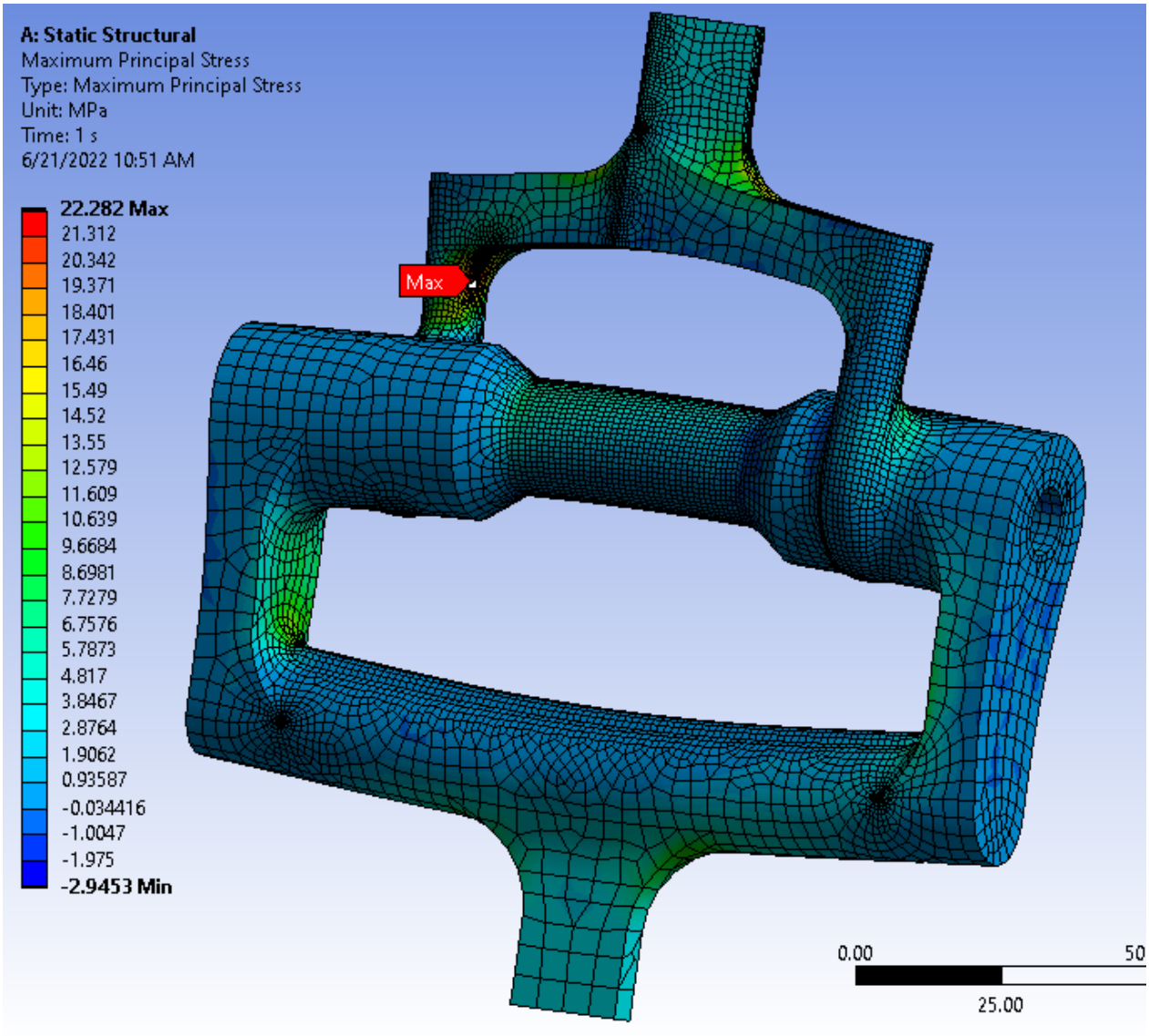

Figure 17: FEA of the first design (colours show the maximum principal stress)

The modelling shows that the greatest maximum stress occurs in the upper handle and not in the testing area as wished. Testing the design however led to failure in the lower handle, where the fillet is fading out (Figure 18).

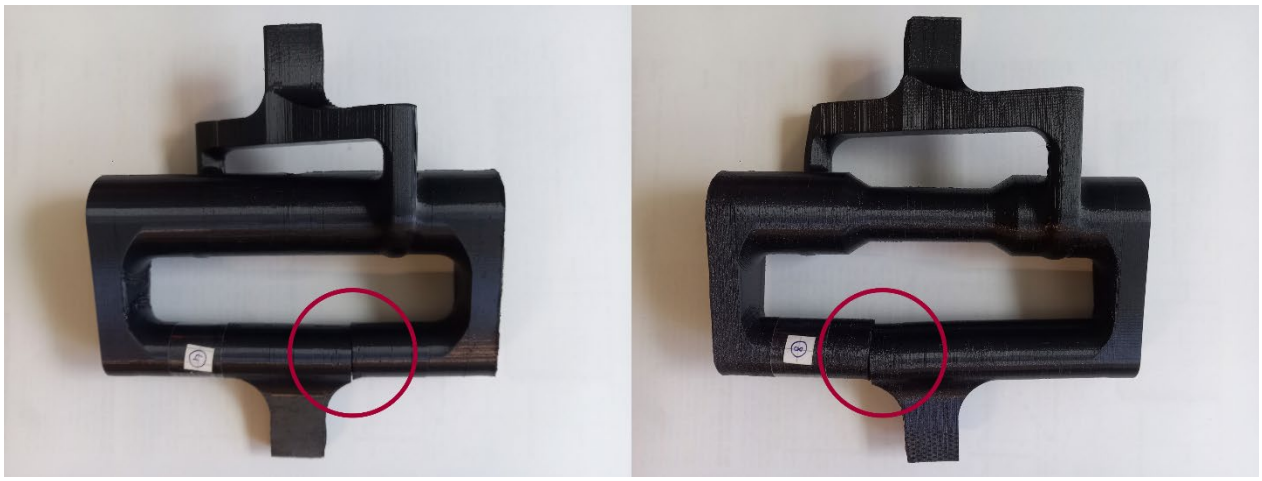

Figure 18: failed first design, No. 4 (left) and No. 8 (right)

To prevent the failure in that part it was made thicker, and after repeated failure it was reinforced with braces (Figure 19), which also failed as shown in Figure 18. Even this was not known then, later findings explain the failure as a printing problem called cracking, which is described in chapter 2.3.2.

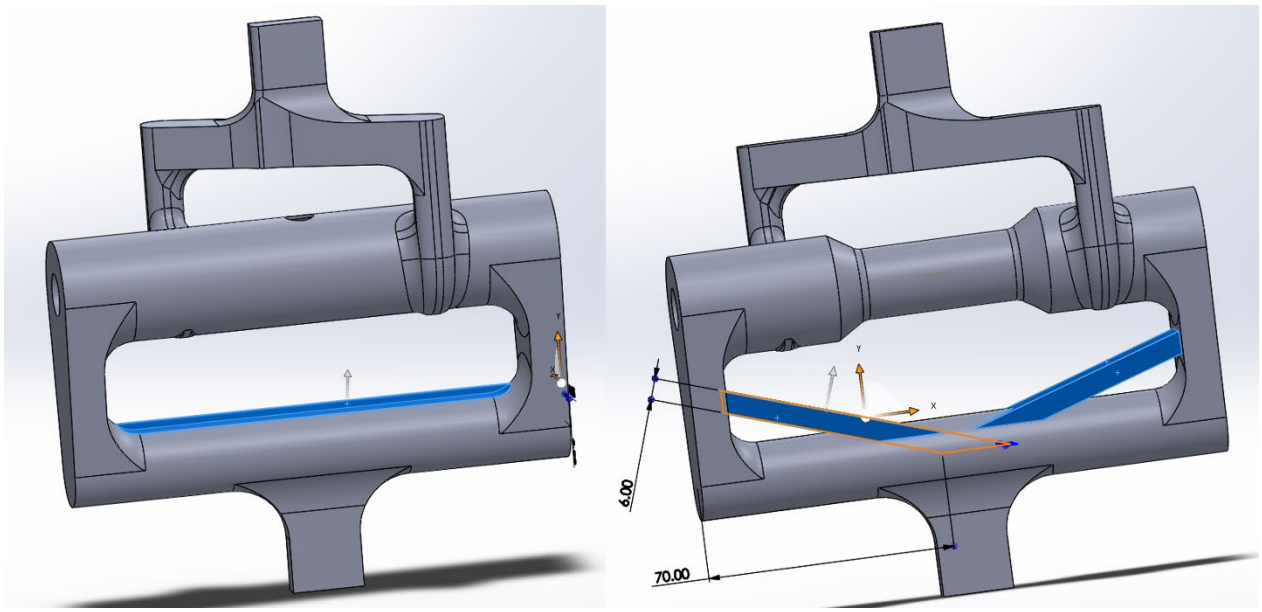

Figure 19: reinforced first design with a stiffener (left) and braces (right)

Due to the failure of this first design, another idea was born, which divided the design into three separate parts (Figure 20). Starting this second design the dimension of the testing area was set fixed and the design was built around it. The length of the testing section is fixed while the diameter and the wall thickness can be adjusted. The dimension of the testing area used in this work are shown in Figure 21. Another second

setting was used with the only change being a wall thickness of 1.0 mm instead of 0.8 mm.

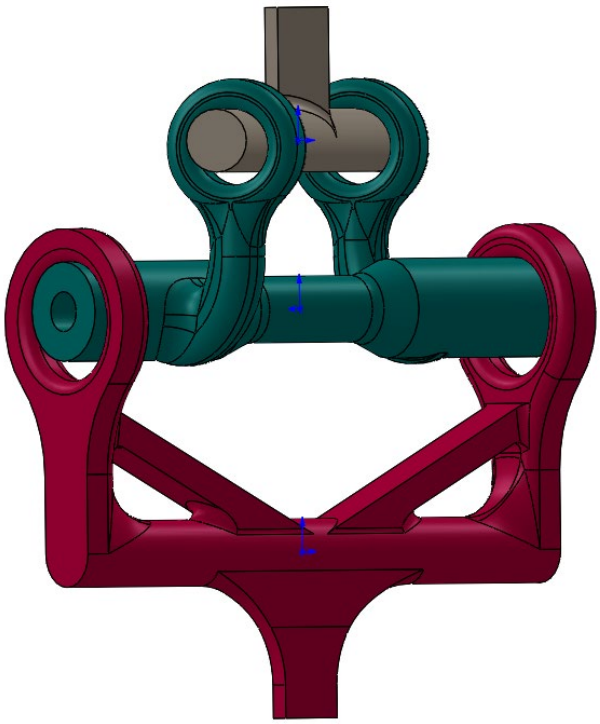

Figure 20: three parts of the second design: upper handle (grey), tube (green) and lower handle (red)

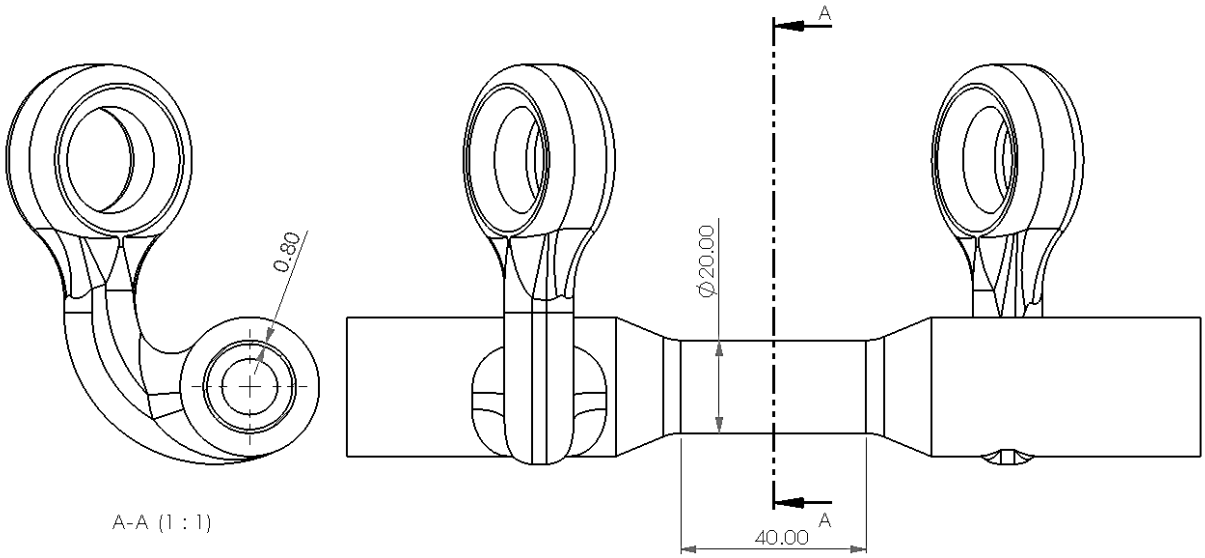

Figure 21: dimension of the testing area

The lower and upper handle now only had to be printed out once as they are merely an extension of the tensile testing machine. The tube now can also move freely along the horizontal axis which eliminates any tension or compression while bending. Another improvement is that the tube now can rotate freely around its centre line. This increases the impact of the torsion, which was rather small in the first design. Another way to increase the impact of the torsion is to make the torsion arm longer (Figure 22). The bending arm on the other hand is at a maximum in this design but can be decreased by shortening the distance between the working point of the upper and the lower handle as shown in Figure 23.

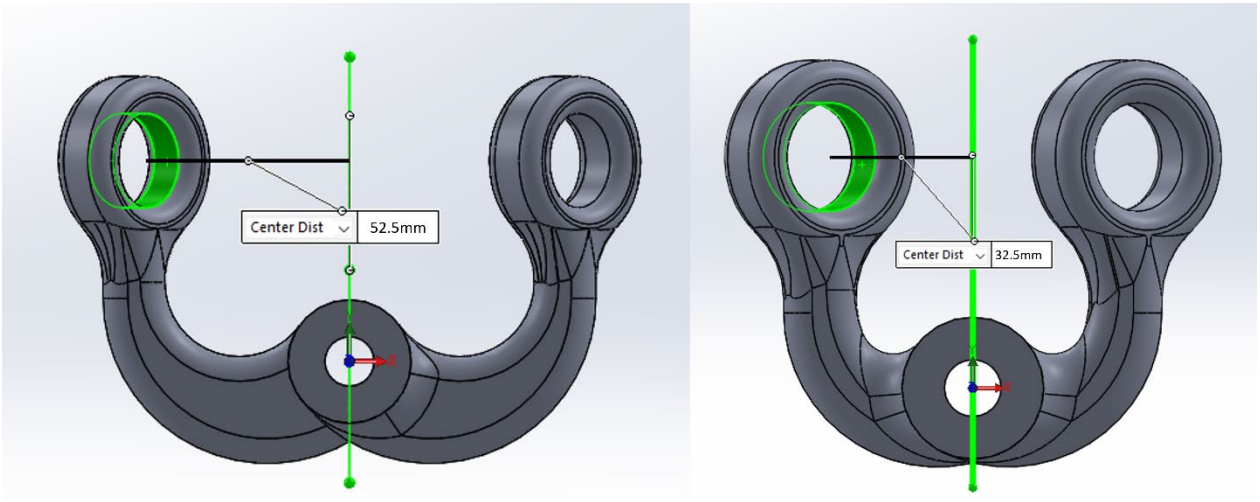

Figure 22: different torsion arms

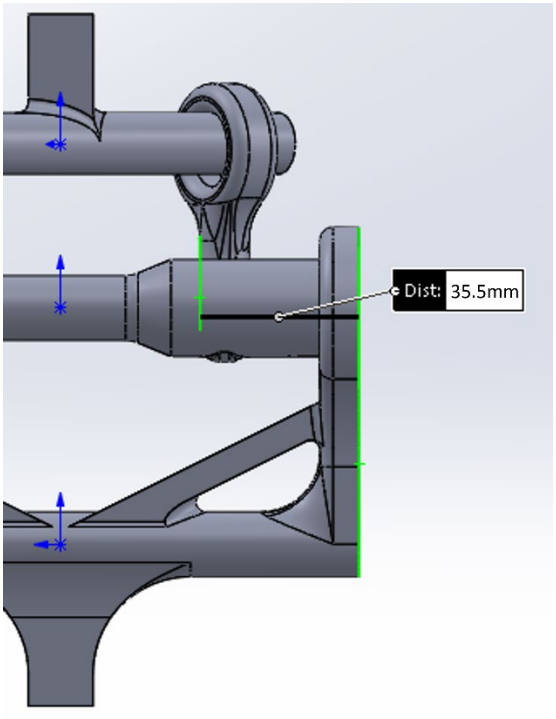

Figure 23: dimension of the bending arm

Printing the lower handle and the tube proved to be a challenge. The prints kept failing as shown in Figure 24. The lower handle was printed out with a crack and the tube was bent. Both failures seemed to be caused by stress along the printing axis (z-axis).

Figure 24: cracked lower handle and bent tube

After some research the failure was identified as cracking. The troubleshooting for this problem is described in chapter 2.3.2. The bending of the tube on the other hand could be fixed by decreasing the distance between the support structure and the actual part in the direction of printing (z-axis). After adjusting a few settings and monitoring the outcomes, the final settings were determined. Using the slicer Ultimaker© Cura 4.13.1 and an Ultimaker© S5 as a printer, the final settings are as shown below. Listed are only the settings that differ from the pre-settings, recommended by the manufacturer.

- filament: black polycarbonate
- 100% infill
- 0.2 mm layer thickness
- Support structure activated
- Using a brim for building plate adhesion
- Line width: 0.4 mm
- Wall line count: 5
- Build volume temperature: 50 °C
- Build plate temperature: 120 °C
- Retraction speed: 40 mm/s
- Support overhang angel: 40
- Minimum support x/y distance: 0.5 mm
- Support z top distance: 0.3 mm
- Brim line count: 10

With these settings all three parts were printed out again and tested together, which was finally successful as the tube failed in the testing section (Figure 25). The outcome of the test was verified again by FEA (Figure 26). Adjusting the printer settings to eliminate cracking took quite some time due to long printing time, so a second path was chosen to ensure the success of this work. The lower and upper handle were 3D printed with aluminium using a Xerox® ElemX™ 3D Printer. This proofed to be a good choice, since the attempt to elimination the cracking seemed successful at first, but the lower handle made from polycarbonate failed after a couple of tests again. Since the material of the lower handle doesn´t have any influence on the testing, the aluminium one was used for all further tests.

Figure 25: successful test (failed tube, No12)

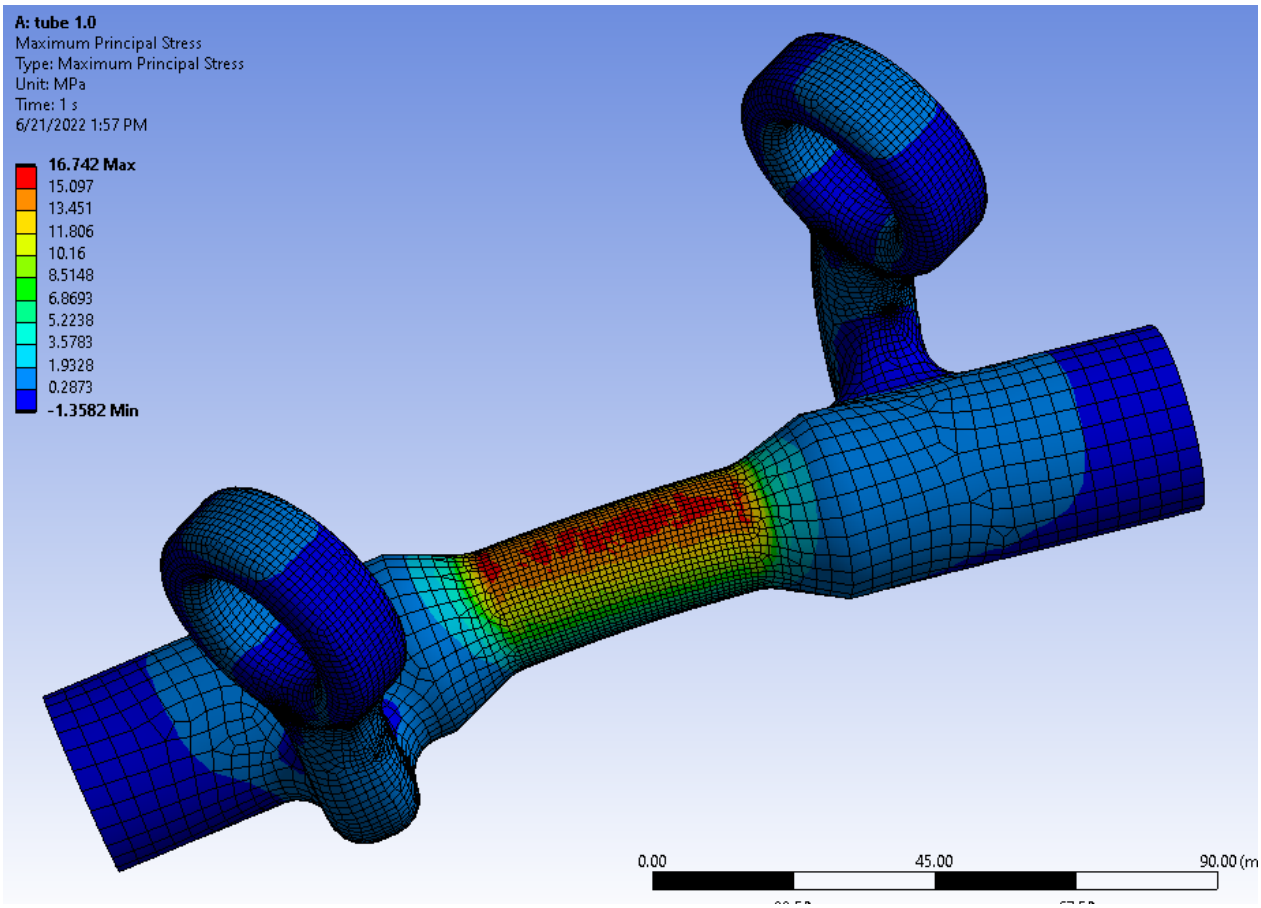

Figure 26: FEA of the tube with applied load

The Ultimaker© 3D-printer is a printer mainly used by amateurs with technological knowledge. Therefore, a lot of settings can be adjusted to provide the user with a wide range of flexibility. Using a professional 3D printer most settings are pre-set by the manufacturer to ensure the success of the print. This leads to less printing time for optimized settings. In addition to the specimens printed out with Ultimaker©, specimens were printed with a Fortus 450mc manufactured by Stratasys, which is designed for industrial use. Due to the different printers, the design had to be adjusted slightly. The Ultimaker© prints with a 0.4 mm nozzle and a layer thickness of 0.2 mm while the Fortus has a 0.2” (0.508 mm) nozzle (T16 tip) and a layer thickness of 0.01” (0.254 mm) [31]. The testing tube formerly having a thickness of 0.8 mm (which is two layers next to each other, as shown in Figure 27) for the Ultimaker©, now had to be adjusted to a 1.0 thickness (still two layers) for the Fortus printer. Testing the design with the industrial manufactured part is the first important step towards industrial testing and production.

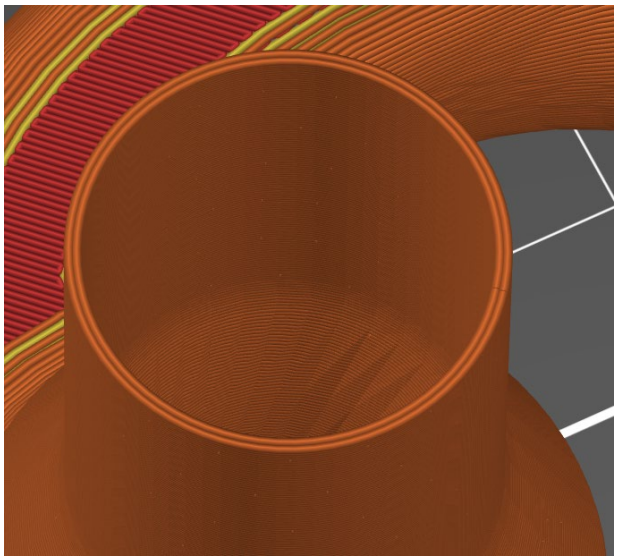

Figure 27: test section, preview of the print, showing the two layers next to each other

4.2.2 Testing

The setup for testing the final design is shown in Figure 28. To secure the tube in the lower handle two caps were used (3D printed). Once the specimen was mounted into the machine the test was started. The settings were again a 2 mm displacement per minute as for the previous tensile tests.

Figure 28: setup for combined loading: PC handles (left) and aluminium handles (right)

In total 16 specimen were tested. Half of them were printed with the Ultimaker© (black polycarbonate), the other ones with the Fortus (white polycarbonate). Both designs have been the same except for the different wall thickness as mentioned in chapter 4.2.1. Four different modifications were tested with two specimens for each of them to verify the results. The first modification was the original design. The second is the same as the first, but with a 6 mm hole drilled into the middle of the upper side of the testing section. The third and fourth are the same as first and second, but with an increased torsion arm. Figure 29 shows all four modifications of the tested tubes.

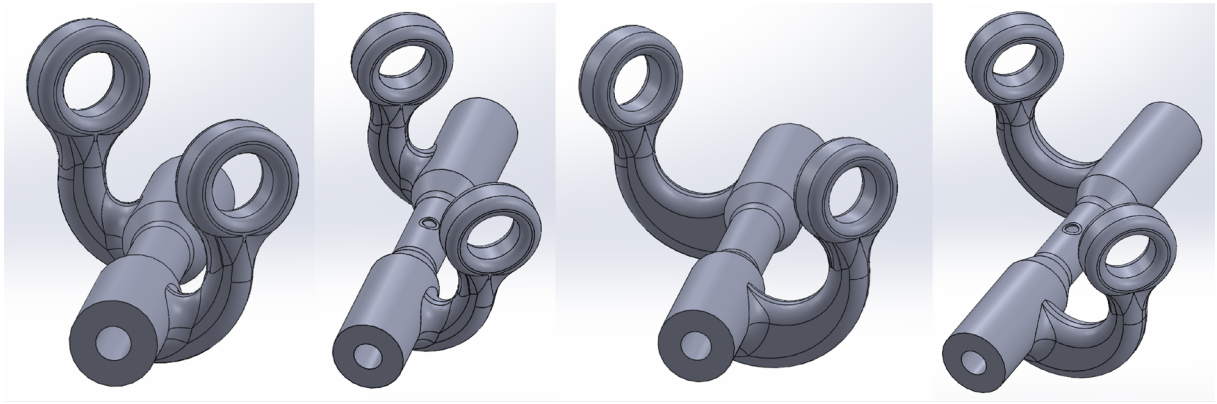

original no hole	original hole	greater torsion no hole	greater torsion hole
0.8: 12 + 13	0.8: 16 + 17	0.8: 20 + 21	0.8: 18 + 19
1.0: F1 + F2	1.0: F3 + F4	1.0: F6 + F7	1.0: F8 + F9

Figure 29: tube modifications

4.2.3 Test results and failure prediction

The test results for the specimens without hole are already shown in Figure 25 and Figure 26. The experimental test matches the simulation as desired. Figure 30 shows the test results for the specimens with a hole and the FEA in comparison. Again, both match as the failure occurs in the test area, where the greatest principal stress appears.

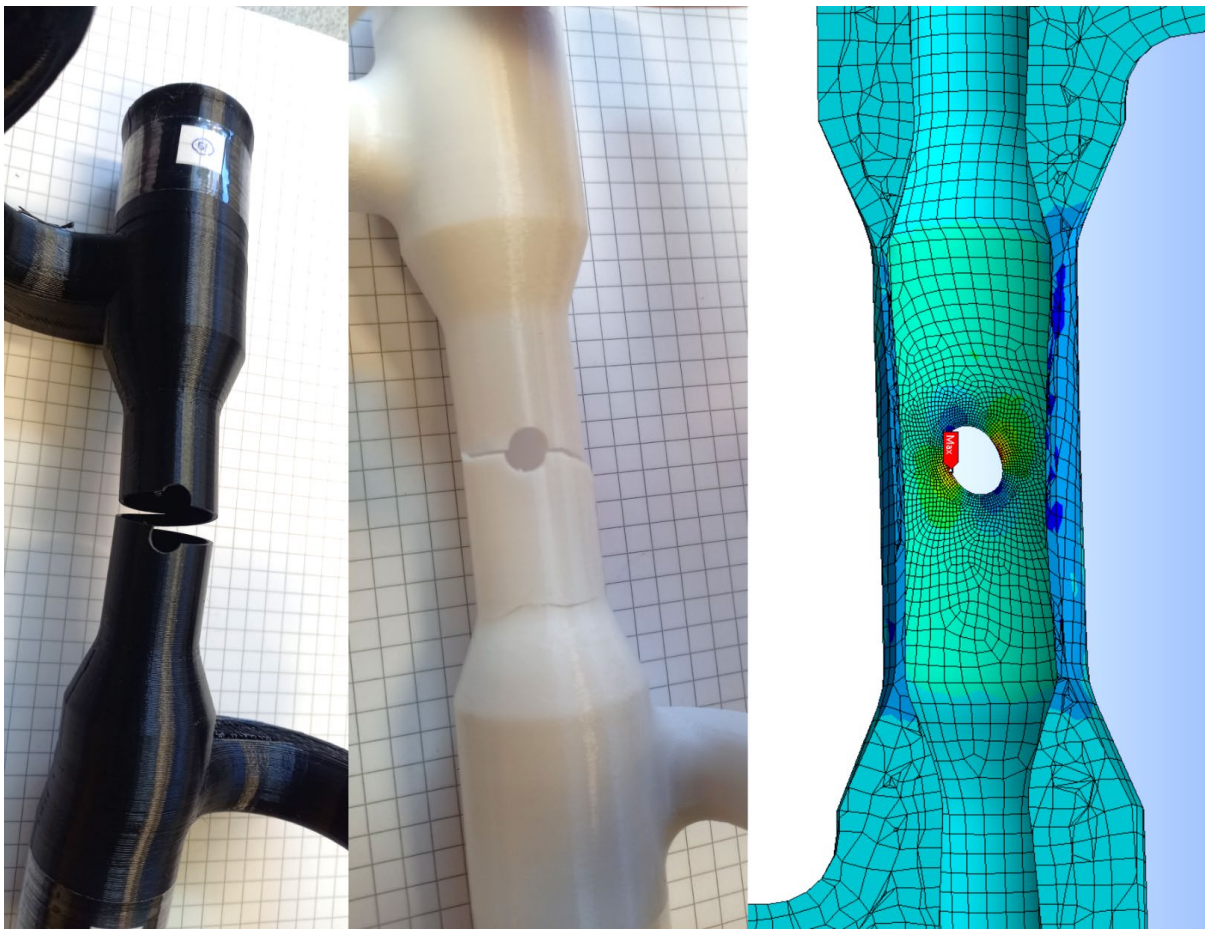

Figure 30: FEA comparing with actual test

The first aim was to verify the data generated by FEA using the software Ansys. This was achieved by comparing the value of the maximum principal stress of FEA with the analytic calculation described in chapter 2.5. To create a mesh for FEA a “hexa dominant” method (dividing the part into cubical finite elements) was chosen with an element size of 0.5 mm in the testing area. For the analytic calculation the bending arm was 35.5 mm (Figure 22) and the two different torsion arms were 32.5 mm and 52.5mm. Table 4 shows the result for both methods and their comparison.

Table 4: maximum principal stress, analytic calculation vs. FEA

	sample	σ_{max} [MPa] (analytic)	σ_{max} [MPa] (FEA)	error [%]
original no hole	No12	44,18	46,85	6,04
	No13	36,26	38,45	
	F1	66,23	71,62	8,14
	F2	78,66	85,07	
greater torsion no hole	No20	49,20	54,70	11,19
	No21	49,91	55,50	
	F6	69,19	82,56	19,33
	F7	68,14	81,31	

The material properties for the material setup in Ansys were determined by testing the black 3D printed polycarbonate as described in chapter 4.1. They were also used for the FEA of the white polycarbonate specimens, which have a slightly different Young´s modulus (black: 1500 MPa, white: 1100 MPa). This explains the higher error value of the white (F1, F2, F6 and F7) specimens compare to the black ones (No12, 13, 20 and 21). This simplification was used, because the printer settings for the Fortus don´t allow the necessary adjustments needed for determining the material properties. But by comparing the analytic calculation with the FEA for **both** materials, the results are similar enough to verify the FEA for further use.

The next steps were used to verify the failure criteria introduced in chapter 0. With the criteria the potential failure location and the failure path are supposed to be predictable. Taking a closer look on the crack and comparing it with FEA both criteria seem to be matched (Figure 31). First a potential failure location is found at the point of the greatest principal stress (first criterion). Second the failure path follows (starting from the potential failure location) the direction of the least value of the left side of equation (15),

being the ratio between the cubic failure stress and the stress gradient along the failure path.

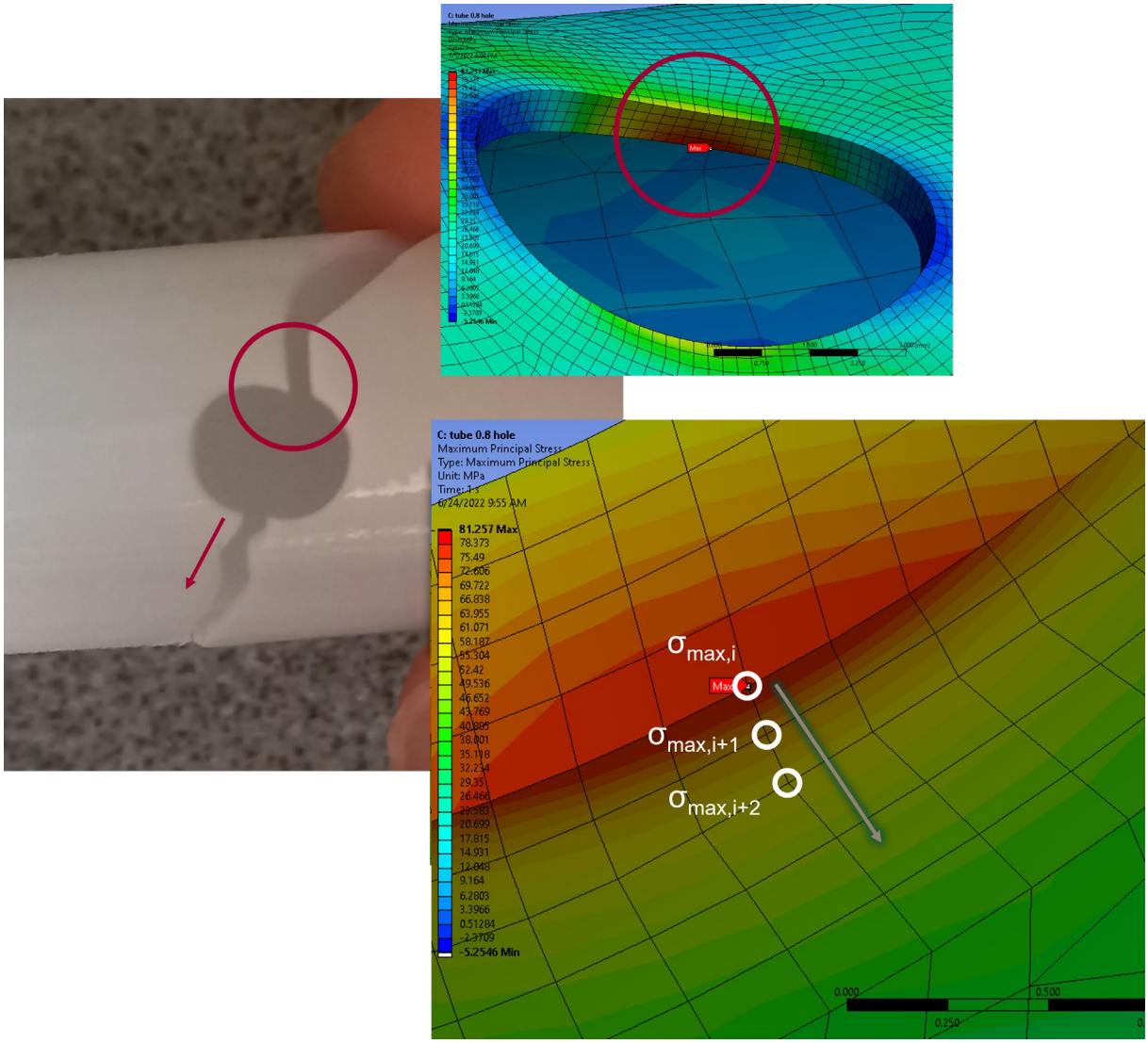

Figure 31: location of the greatest maximum principal stress and the direction used for calculation the stress gradient

Comparing the failure stress of the specimens with and without hole, the fact that both criteria must be met is proved as well. For both torsion arms and both materials the failure stress of the sample without hole is smaller than the ones with hole (Figure 32). If only the first criterion had to be met, the specimens with a hole would fail at the same stress as the ones without hole. But they can endure a way greater stress, because the second criterion has to be met as well.

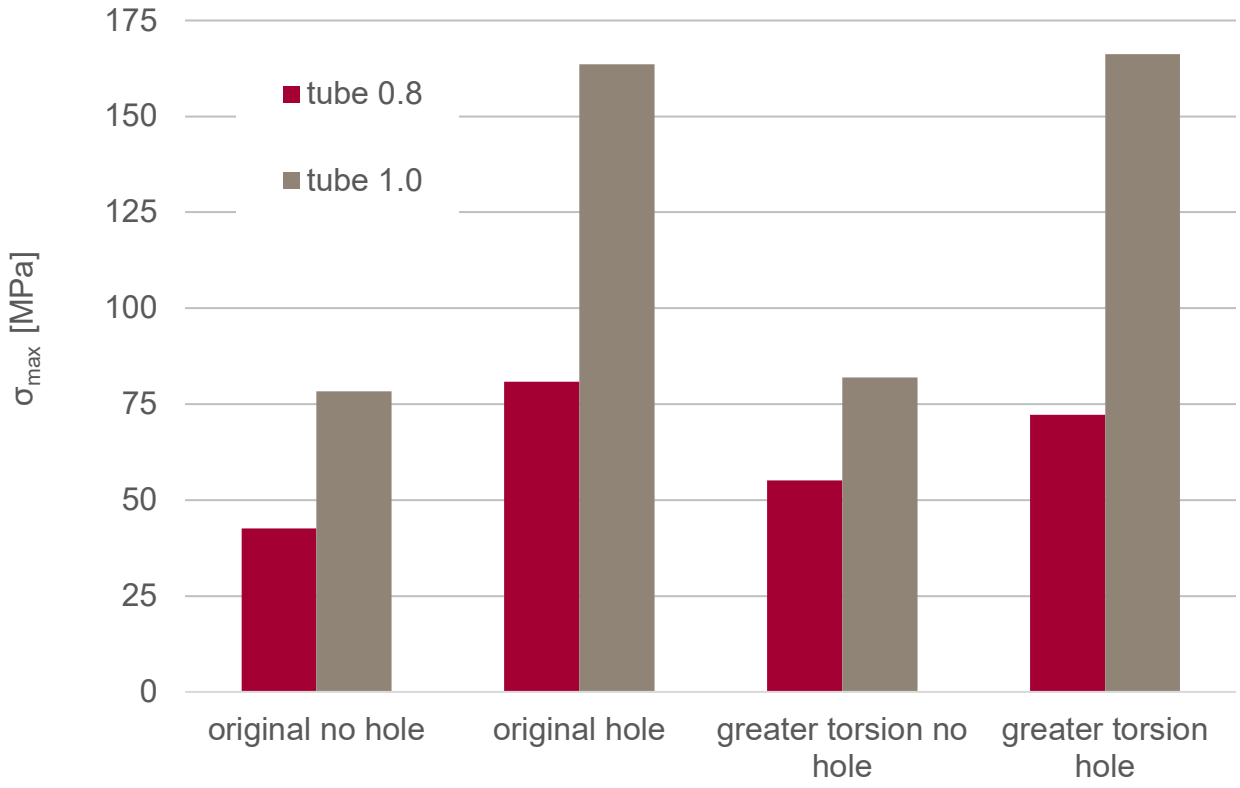

Figure 32: comparing the failure stress with and without hole

The last step for verifying the failure criterion is to find the failure value for both materials so the failure stress can be predicted. Using the second criterion, the failure stress was predicted by using the stress gradient, which was determined by starting at the point of the greatest maximum principal stress and moving along the failure path. Comparing the prediction with the experimental data for each material a failure value could be found to match the different loadings (original and increased torsion) as shown in Table 5.

Table 5: stress gradient, failure stress and value (experimental and prediction)

	σ_{max} [MPa]					
	experimental	**average**	**prediction**	**χ [1/m]**	**$2E\kappa_{fail}$ [MPa²mm]**	**error [%]**
F3	157,58	163,57	164,60	743,25	6000	0,63
F4	169,55					
F8	174,35	166,17	166,51	769,47	6000	0,20
F9	158,00					
No16	94,58	80,85	76,55	773,40	580	-5,32
No17	67,13					
No18	79,42	72,18	76,01	757,08	580	5,30
No19	64,95					

5 Summary and outlook

Both goals for this work have been achieved. The first one was to find and print a design for combined loading (bending and torsion) while applying uniaxial load. The 2nd design with its three parts and variable test section proved to be able to apply torsion and bending at the same time under uniaxial loading to the test section. The way the test section failed and the different failure load for the different torsion arms are again evidence for the success of the design. Even though the designing was a major part of this work it was “only” an essential step to prove that the introduced failure criteria are applicable not only for uniaxial loading but for combined loading also. The theory states that both criteria must be met which was demonstrated as the specimens without hole failed at a lower stress than the ones with a hole, exceeding the failure strength of the material by far. In addition, the failure location and path could be predicted using the stress gradient and FEA, which matched the actual cracks in the specimen. Finally, a failure value could be found specific to each material to match the experimental failure stress with the predicted one. This leads to the conclusion that the failure criteria are applicable to combined loading as well.

Since a major part of this thesis was the designing of a specimen, further testing should be done to verify the failure criteria. The dimensions of the testing area as well as the proportion of bending and torsion can be also modified and tested to increase the database. But most importantly 3D-printing allows a nearly unlimited variety of designs for whichever combined loading might appear or will be desired. With the ability to predict failure for combined loading now, the use of 3D-printed components will be safer, more reliable and even applicable for safety related spare parts as needed on board of warships.

6 List of figures

7 List of tables

8 Literaturverzeichnis

[1] JACK COLYER: *U.S. NAVY EXPANDS ITS METAL 3D PRINTING CAPABILITIES*. URL https://3dprintingindustry.com/news/u-s-navy-expands-its-metal-3d-printing-capabilities-157039/ – Access date 23.06.22

[2] LARS HOFFMANN: *Bundeswehr lotet Potenzial für 3D-Druck aus*. URL https://esut.de/en/2021/11/meldungen/30838/bundeswehr-lotet-potenzial-fuer-3d-druck-aus/ – Access date 20.03.2022

[3] JOSEPH R. DAVIS: *Tensile Testing*. 2nd. Ohio, USA : ASM International, 2004

[4] YASIN ÇAPAR: *Engineering Stress/Strain vs True Stress/Strain*. URL https://yasincapar.com/engineering-stress-strain-vs-true-stress-strain/ – Access date 19.06.2022

[5] ZAINUL HUDA, Robert Bulpett: *Material sience and design for engineers*. Zurich-Durnten, Switzerland, Enfield, New Hampshire : Trans Tech Publications, 2012

[6] LIM, Hanpin ; HOAG, Stephen: *Plasticizer Effects on Physical–Mechanical Properties of Solvent Cast Soluplus® Films*. In: *AAPS PharmSciTech* 14 (2013)

[7] GRANT MALOY SMITH: *Wie man Dehnung und Druck mit Dehnungsmessstreifen misst*. URL https://dewesoft.com/de/daq/dehnung-und-druck-messen#poisons-ratio – Access date 20.06.22

[8] TED NACHAZEL: *What is a Strain Gauge and How Does it Work?* URL https://www.michsci.com/what-is-a-strain-gauge/

[9] MICROMEASUREMENTS: *General Purpose Strain Gages—Tee Rosett*. URL https://docs.micro-measurements.com/?id=2554 – Access date 20.06.22

[10] MICROMEASUREMENTS: *What is a Strain Gage?* URL https://micro-measurements.com/what-is-a-strain-gage – Access date 20.06.22

[11] JACOB SEGIL (Hrsg.): *Handbook of Biomechatronics* : Academic Press, 2019

[12] MARTIN BATES (Hrsg.): *Interfacing PIC Microcontrollers (Second Edition)*. Second Edition. Oxford : Newnes, 2014

[13] VICTOR GIURGIUTIU (Hrsg.): *Structural Health Monitoring of Aerospace Composites*. Oxford : Academic Press, 2016

[14] SAXENA, Vimal (Hrsg.); KRIEF, Michel (Hrsg.); ADAM, Ludmila (Hrsg.): *Handbook of Borehole Acoustics and Rock Physics for Reservoir Characterization* : Elsevier, 2018

[15] RAFIQ NOORANI: *3D Printing: Technology, Applications, and Selection*. In: *MRS Bulletin* 43 (2018), Nr. 6, S. 462. URL https://www.cambridge.org/core/article/3d-printing-technology-applications-and-selection-by-rafiq-noorani/7CC2BAFFAA04128486D8E1CF5E24BC0C

[16] JORDAN, John M.: *3D printing*. Cambridge : MIT Press, 2019 (MIT Press essential knowledge series)

[17] ADDITIVELY: *Fused Deposition Modeling*. URL https://www.additively.com/de/lernen/fused-deposition-modeling – Access date 07.11.2019

[18] ULTIMAKER: *How to store material*. URL https://support.ultimaker.com/hc/en-us/articles/360012101319-How-to-store-material. – Aktualisierungsdatum: 2022-05-09 – Access date 20.06.22

[19] *Warping and Cracking with closed environment FDM3D printers*. URL https://www.box3d.eu/warping-cracking-closed-environment-3d-printers/ – Access date 20.06.22

[20] MATT TYSON: *Warp free polycarbonate (PC) 3D printing is here!* URL https://www.3dprintingsolutions.com.au/News/Australia/warp-free-polycarbonate-pc-3d-printing-is-here – Access date 20.06.22

[21] PANAYIOTIS PAPADOPOULOS: *Introduction to the Finite Element Method*. URL https://csml.berkeley.edu/Notes/ME280A.pdf – Access date 23.06.22

[22] KARAN KUMAR PRADHAN (Hrsg.); SNEHASHISH CHAKRAVERTY (Hrsg.): *Computational Structural Mechanics* : Academic Press, 2019

[23] KWON, Young ; DIAZ-COLON, Carlos ; DEFISHER, Stanley: *Failure Criteria for Brittle Notched Specimens*. In: *Journal of Pressure Vessel Technology* 144 (2022)

[24] CUAN-URQUIZO, Enrique ; BAROCIO, Eduardo ; TEJADA-ORTIGOZA, Viridiana ; PIPES, Byron ; RODRIGUEZ, Ciro ; ROMAN-FLORES, Armando: *Characterization of the Mechanical Properties of FFF Structures and Materials: A Review on the*

Experimental, Computational and Theoretical Approaches. In: *Materials* 12 (2019), S. 895

[25] PUIGORIOL, J. M. ; ALSINA, Alex ; SALAZAR MARTÍN, Antonio Gabino ; GÓMEZ-GRAS, Giovanni ; PÉREZ, Marco: *Flexural Fatigue Properties of Polycarbonate Fused-deposition Modelling Specimens*. In: *Materials & design* 155 (2018), S. 414–421

[26] CANTRELL, Jason ; ROHDE, Sean ; DAMIANI, David ; GURNANI, Rishi ; DISANDRO, Luke ; ANTON, Josh ; YOUNG, Andie ; JEREZ, Alex ; STEINBACH, Douglas ; KROESE, Calvin ; IFJU, Peter: *Experimental characterization of the mechanical properties of 3D-Printed ABS and polycarbonate parts*. In: *Rapid Prototyping Journal* 23 (2017)

[27] SLÁMECKA, K. ; POKLUDA, J.: *Simple criterion for predicting fatigue life under combined bending and torsion loading*. In: *Frattura ed integritá strutturale* 11 (2017), Nr. 41, S. 123–128. URL https://www.researchgate.net/publication/318583321_Simple_criterion_for_predicting_fatigue_life_under_combined_bending_and_torsion_loading

[28] GREGORI, J. Navarro ; SOSA, P. Miguel ; PRADA, M. A. Fernández ; FILIPPOU, Filip C.: *A 3D numerical model for reinforced and prestressed concrete elements subjected to combined axial, bending, shear and torsion loading*. In: *Engineering Structures* 29 (2007), Nr. 12, S. 3404–3419. URL https://www.sciencedirect.com/science/article/pii/S0141029607003604

[29] MUDUNURU, Maruti Kumar ; PANDA, Nishant ; KARRA, Satish ; SRINIVASAN, Gowri ; CHAU, Viet T. ; ROUGIER, Esteban ; HUNTER, Abigail ; VISWANATHAN, Hari S. ; LOS ALAMOS NATIONAL LAB. LOS ALAMOS, NM: *Surrogate Models for Estimating Failure in Brittle and Quasi-Brittle Materials*. In: *Applied sciences* 9 (2019), Nr. 13, S. 2706. URL https://www.researchgate.net/publication/334208890_Surrogate_Models_for_Estimating_Failure_in_Brittle_and_Quasi-Brittle_Materials

[30] URL material properties — Ansys Learning Forum – Access date 19.05.22

[31] STRATASYS: *Operation and Maintenance Guide Fortus 380mc/450mc*. URL https://www.stratasys.com/-/media/files/documentation/fdm/Fortus-380mc-and-

450mc-K6K1-Series/Operation-Guide/380_450_Operation%20and%20Maintenance_REV_A.pdf – Access date 20.06.22

Appendix

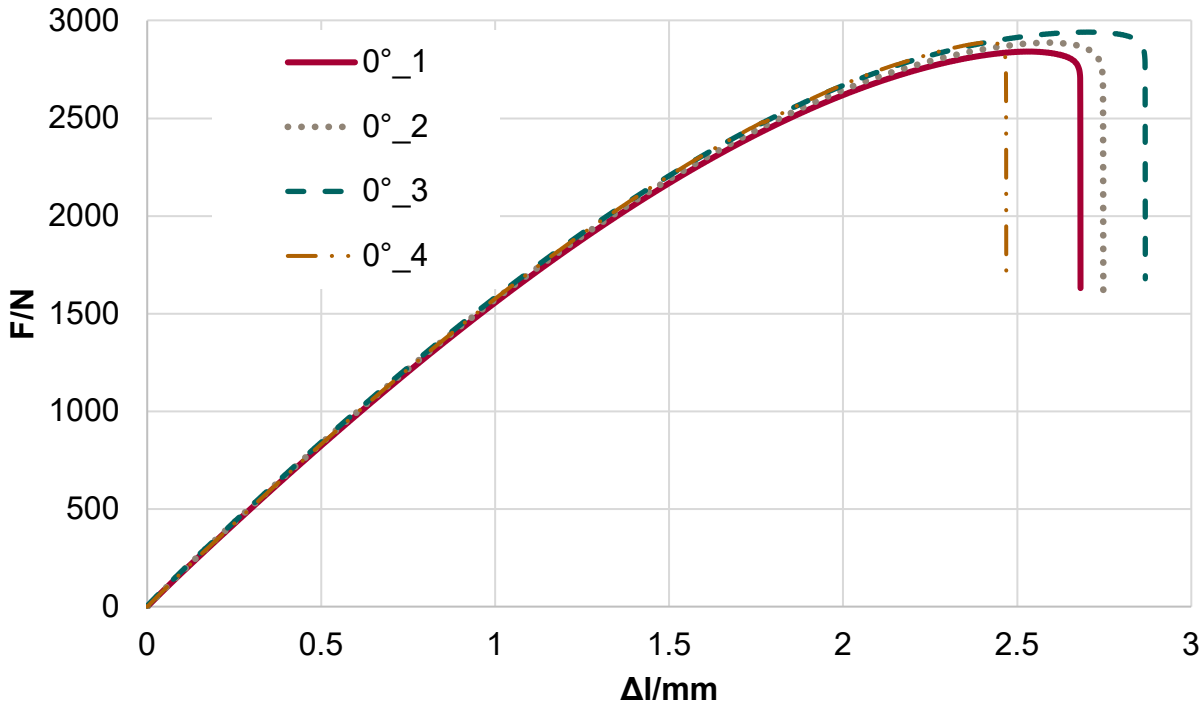

Figure 33: stress-strain-curve for 0° printed specimen

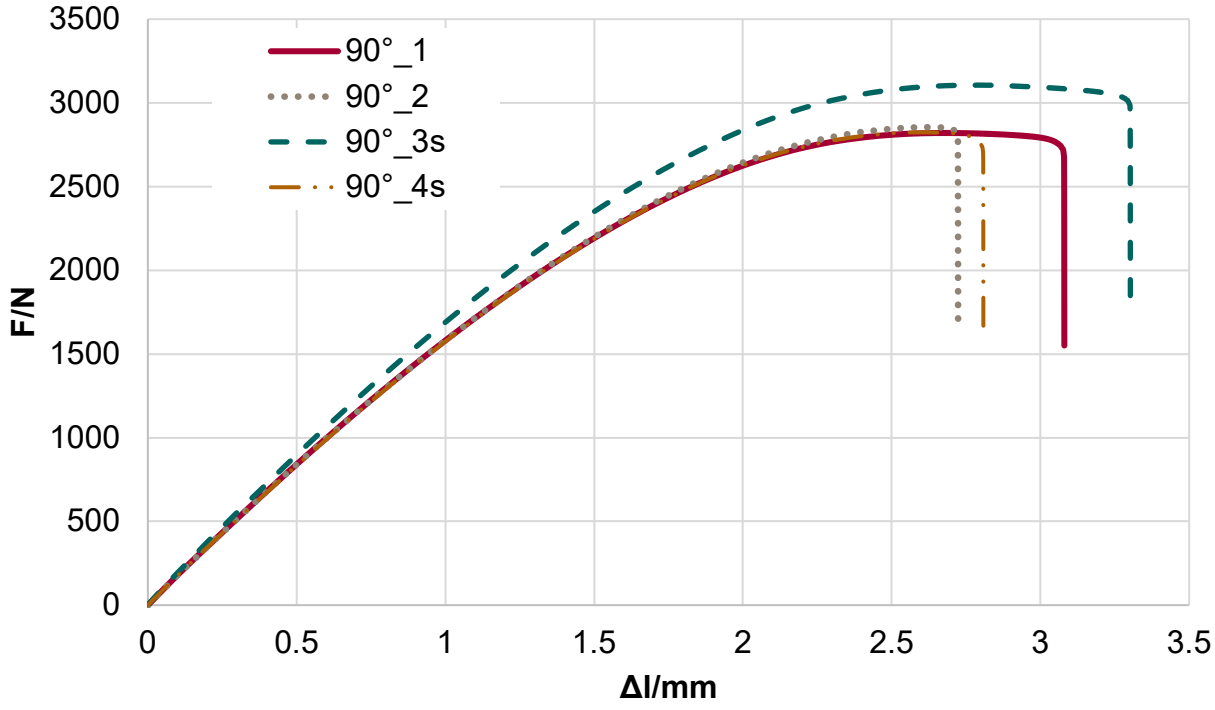

Figure 34: stress-strain-curve for 90° printed specimen

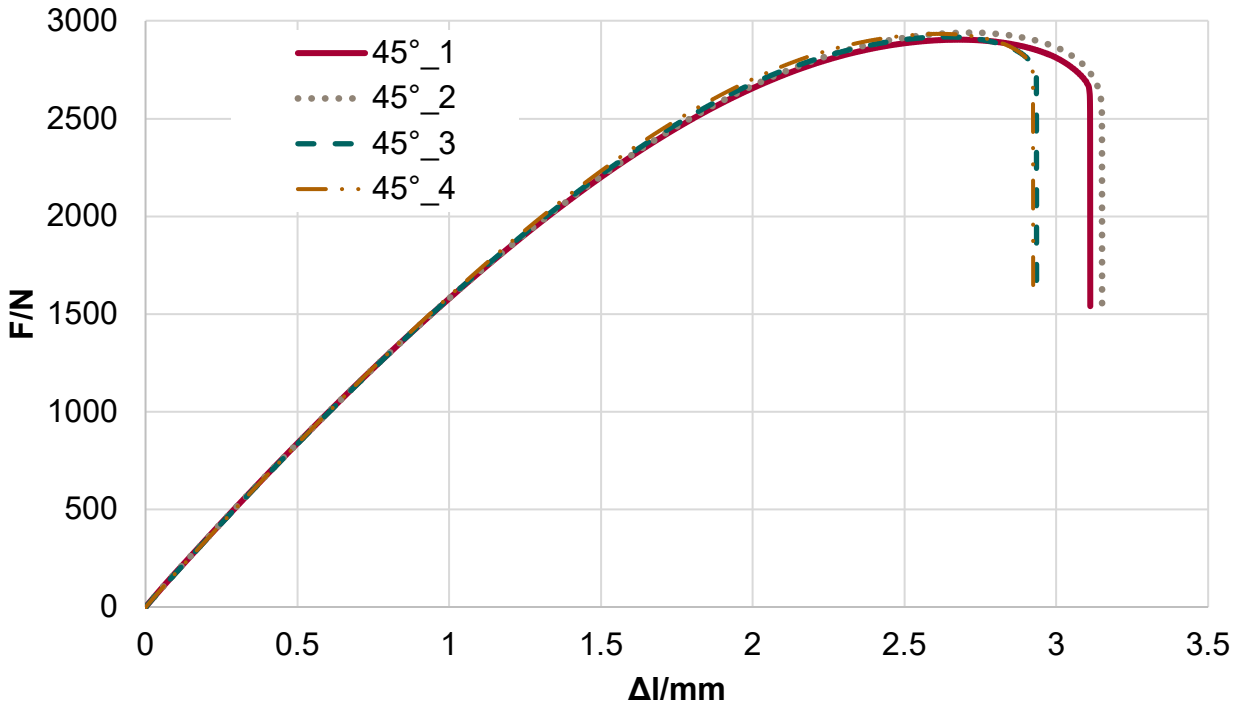

Figure 35: stress-strain-curve for 45° printed specimen

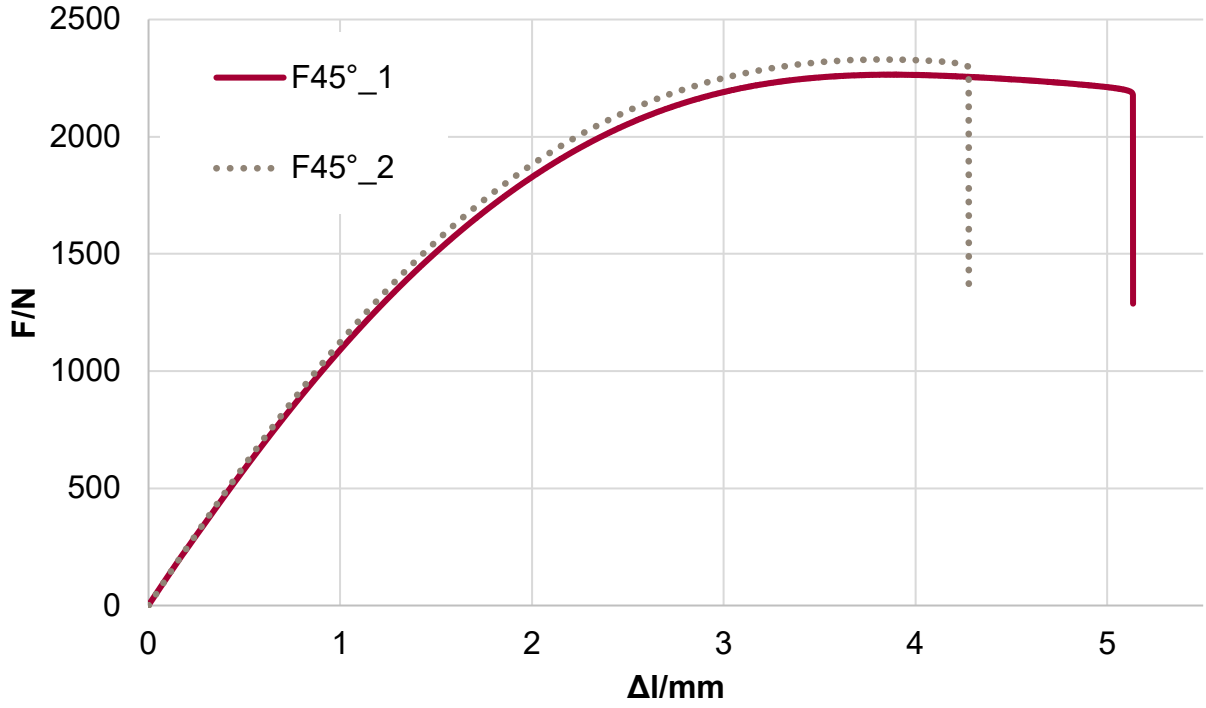

Figure 36:stress-strain-curve for 45° printed specimen with the Fortus 450mc

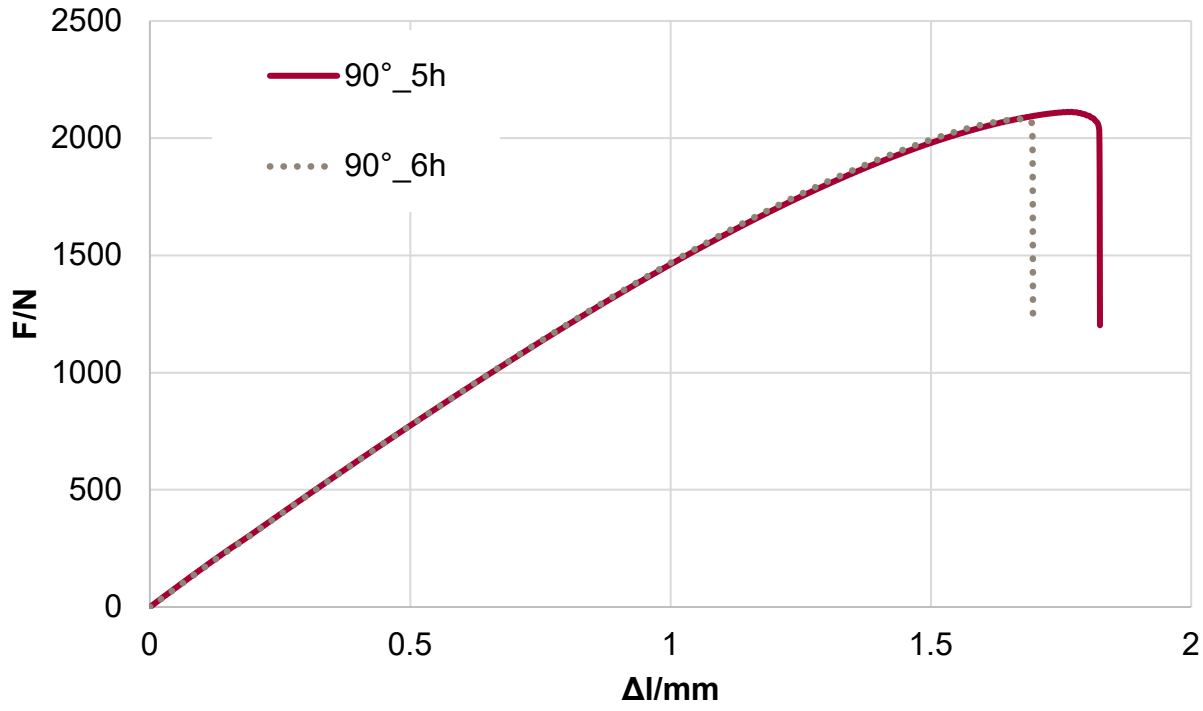

Figure 37:stress-strain-curve for 90° printed specimen with a 6 mm hole

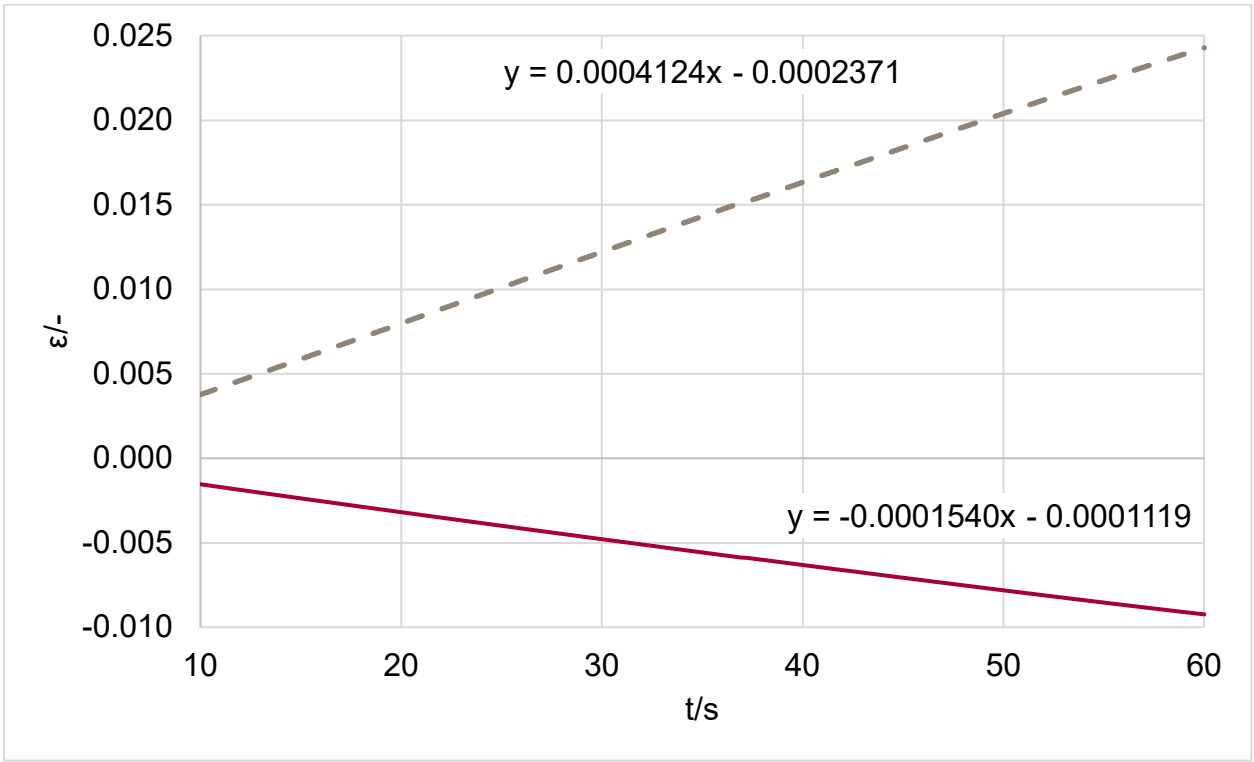

Figure 38: strain gauges result for 0°_3, showing the longitudinal (grey, broken curve) and transversal (red) strain

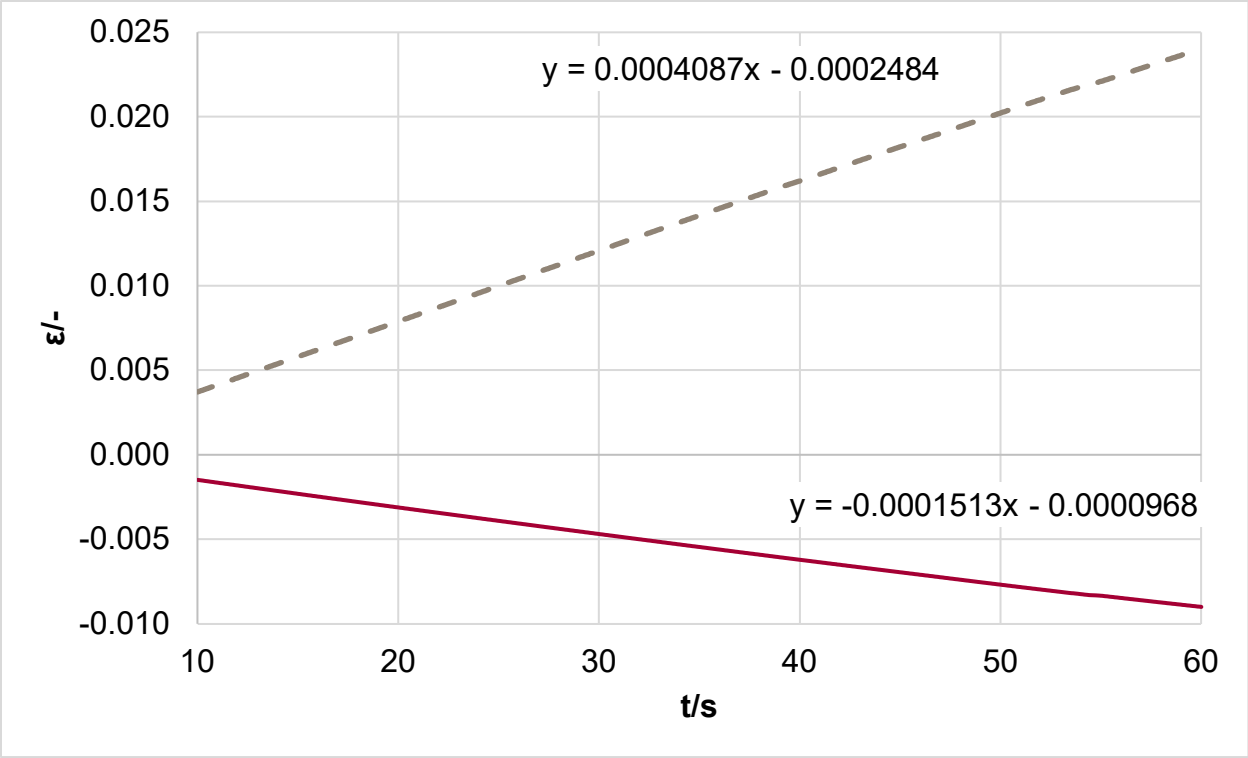

Figure 39: strain gauges result for 0°_4, showing the longitudinal (grey, broken curve) and transversal (red) strain

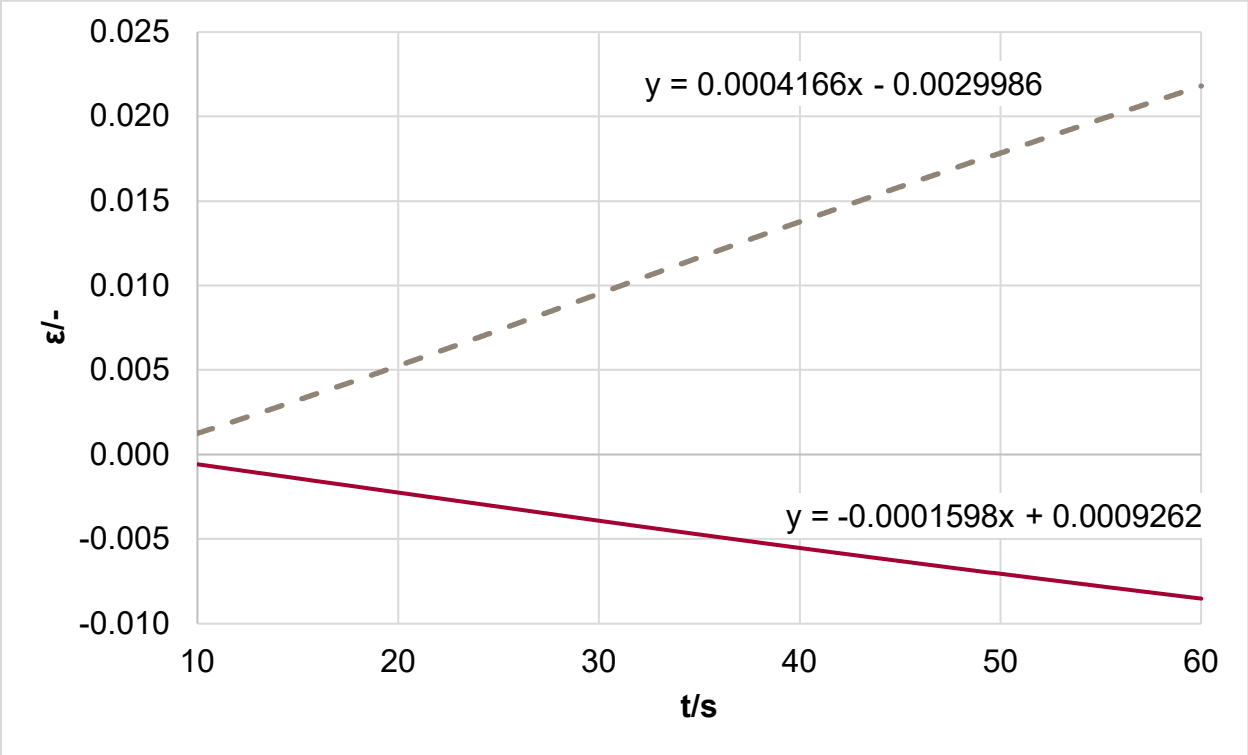

Figure 40: strain gauges result for 90°_3, showing the longitudinal (grey, broken curve) and transversal (red) strain

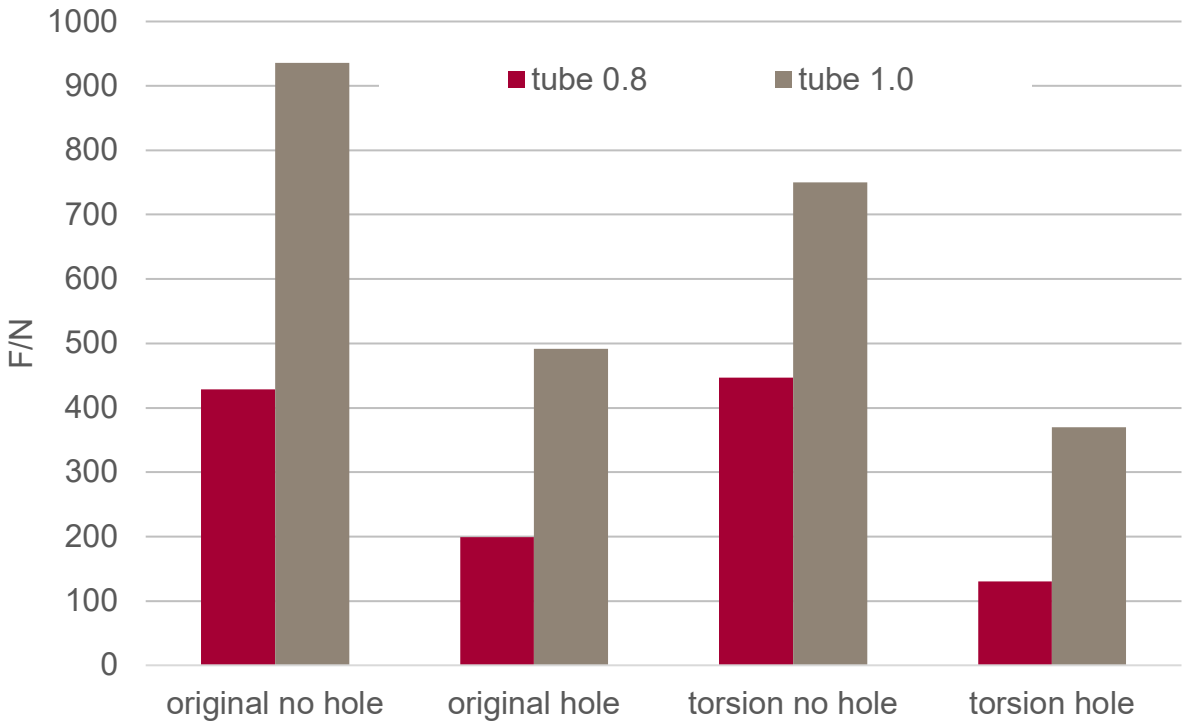

Figure 41: failure stress

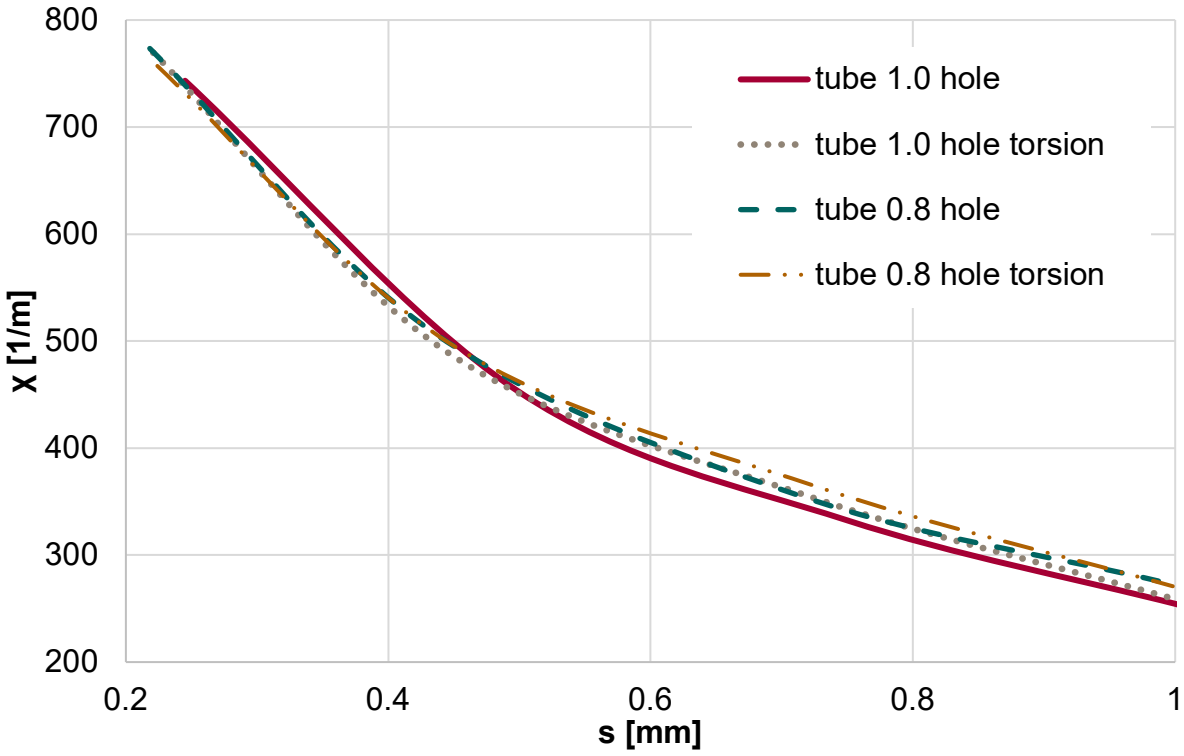

Figure 42: Stress gradient

Declaration of authorship/Eigenständigkeitserklärung

Hiermit erkläre ich, die Master-Thesis mit dem Thema: „Entwerfen und Testen eines 3D-gedruckten Prüfkörpers für überlagerte Beanspruchung“ selbstständig und ohne fremde Hilfe verfasst zu haben. Des Weiteren versichere ich, dass ich die Arbeit bisher weder an der Helmut-Schmidt-Universität/Universität der Bundeswehr Hamburg noch an einer anderen Hochschule eingereicht habe. Alle Stellen, die wörtlich oder sinngemäß aus Veröffentlichungen anderer entnommen sind, habe ich als solche kenntlich gemacht. Diese Versicherung gilt auch für alle der Arbeit beigegebenen Zeichnungen, Skizzen, Abbildungen etc.

Monterey, den 14.07.2022 Unterschrift: